Chapter 7
Ab Initio Thermodynamics and First-Principles Microkinetics for Surface Catalysis

Karsten Reuter

Abstract Ab initio thermodynamics and first-principles microkinetic simulations have become standard tools in research on model catalysts. Complementing dedicated in situ experiments, these techniques contribute to our evolving mechanistic understanding, in particular of a reaction-induced dynamical evolution of the working catalyst surface. This topical review surveys the methodological foundations and ongoing developments of both techniques, and specifically illustrates the type of insights they provide in the context of in situ model catalyst studies. This insight points at substantial deviations from the standard picture that analyzes catalytic function merely in terms of properties of and processes at active sites as they emerge from a crystal lattice truncation of the nominal catalyst bulk material.

7.1 Introduction

An obvious target of research in heterogeneous catalysis is to develop "better" catalysts. "Better" may thereby stand for quite different aspects. Among others this can be higher activity, higher selectivity, longer lifetimes, or preferable materials. Whatever the targeted improvements are specifically though, if they are to be found by anything but mindless trial and error, one necessarily needs "ideas". One powerful source of ideas to find better catalysts is to understand what limits the function of existing catalysts. Generally, the better or detailed this understanding is, the better defined are the ideas that emerge from it. This line of thinking is the basic motivation for catalysis research that aims for what one refers to as mechanistic understanding. Here, mechanistic ideally means understanding the function down to the atomistic level of the individual elementary processes that underlie the catalytic

This chapter has also been published as Catalysis Letters 146 (3), 541—563 (2016).

K. Reuter (✉)
Chair for Theoretical Chemistry and Catalysis Research Center, Technical University Munich, Lichtenbergstr. 4, 85747 Garching, Germany
e-mail: karsten.reuter@ch.tum.de

J. Frenken and I. Groot (eds.), Operando *Research in Heterogeneous Catalysis*,
Springer Series in Chemical Physics 114, DOI 10.1007/978-3-319-44439-0_7

cycle. It turns out that this is a pretty daunting goal. One possibility to make it at least a bit more tractable is to reduce the complexity of the problem and achieve this understanding first for model catalysts [1, 2], i.e. typically single-crystals of the actual catalyst material or defined nanoparticles of the material on single-crystal supports. This dismisses many aspects of a real catalyst, and may therefore only generate a subset of ideas—but, one has to make a start.

One of the central, novel aspects that have recently emerged from such mechanistic studies on model catalysts is that an operating catalyst surface could be anything but a static entity [3, 4]. A prevailing view of heterogeneous catalysis often found in introductory textbooks is instead that of impinging and reacting gas-phase species on a rigid solid surface [5–7]. If the atomic structure of the surface is resolved at all in such a picture, then this is the crystallographic structure as resulting from a mere surface truncation of the bulk catalyst lattice. For instance, for metal catalysts one pictures a low-index facet like a (111) or (100) fcc surface, flat like a tablet, at best with some steps in between. The surface metal atoms have a reduced metal coordination in comparison to the coordination of a bulk atom. This makes them "active" and one views particular high-symmetry adsorption sites on the lattice defined by the position of these "active" surface atoms as the ones driving the catalysis. Consequently denoted as "active sites", in the example of the fcc metal surface this could e.g. be hollow, bridge or atop adsorption sites on the terraces, or equivalent sites at upper or lower step edges. The surface metal atoms around these active sites adapt their positions slightly to the ongoing elementary processes of the catalytic reaction, namely adsorption, diffusion, reaction, and desorption of the reactants and reaction intermediates. However, apart from such small structural relaxations, the surface morphology is assumed to be pretty static. As such, the catalytic function is analyzed in terms of the properties of and processes at these active sites, thinking specifically of sites as they emerge from the crystal lattice truncation of the nominal catalyst bulk material.

While seductively familiar and intuitive, this picture could fall short in capturing much of real heterogeneous catalysis. For sure, the picture is largely correct in the defined environment offered by controlled gas dosage in ultra-high vacuum (UHV) and at low temperatures. Most of what we know on an atomic level about surface catalytic reactions derives from such environments and this is why the above sketched picture is familiar and intuitive to us. However, heterogeneous catalysis does not operate in UHV. Technologically relevant gas-phase conditions comprise ambient pressures or beyond. Under a corresponding, much fiercer gas-phase impingement we at least have to expect increased adsorbate concentrations at the surface and concomitantly higher reaction rates, typically measured in turnover frequencies (TOF) with units of product molecules per catalyst surface area and time. If this was all, it should still be possible to extrapolate from UHV to ambient conditions and to slow things down by studying lower temperatures. Such "thermodynamic scaling" (vide infra) was the original hope or assumption of the Surface Science approach to Heterogeneous Catalysis. Increasingly, we are able to scrutinize this assumption. This is made possible by the advent of so-called in situ studies that investigate model catalysts at ideally similar atomic resolution as in

traditional UHV Surface Science, but at (near-)ambient pressures [8, 9]. What we have learnt from such studies so far, sketches a picture of heterogeneous catalysis that goes far beyond a simple thermodynamic scaling.

For instance, the surface concentrations of certain reaction intermediates can become so high that phase transitions to new compound materials composed of the original (nominal) catalyst material and the reaction intermediate may occur—and it is this new material that then actuates the catalysis [4, 8, 9]. Both for thermodynamic or kinetic reasons these new materials must furthermore by no means be restricted to known bulk phases. Instead they can exhibit completely new structures that are (temporarily) stabilized for instance as thin surface films on top of the bulk catalyst. A prominent example for such surface morphological transitions is oxide formation at the late transition metals employed in oxidation catalysis [10–14]. Another aspect that speaks against a simple scaling from UHV to ambient pressures is the much higher amount of reaction energy that is released in case of exothermic reactions at the increased reaction rates. We presently know very little about how and how quickly this energy is dissipated on an atomic-scale [15]. Yet, if heat transfer is limited, scenarios like molten catalyst materials with a surface dynamics much beyond that of rigidly lattice-aligned active sites are well conceivable.

One needs to stress that the current understanding we have gained through in situ studies is far from being complete; Certainly much less than what we have collected in decades of UHV Surface Science work. At present it is not clear whether those instances reported are exotic oddities or the top of the iceberg. The data we already have is nevertheless good enough to formulate a working hypothesis opposite to the prevalent static picture: Why not view a catalyst surface as something entirely dynamic? A surface that while operating adapts sensitively to the reaction conditions in everything ranging from the local atomic structure to overall composition and morphology? Yes, new surface phases can form in the reactive gas-phase, but why should they always cover the entire catalyst surface? As a result, if the surface is then heterogeneous, why should this surface heterogeneity not vary with time? Maybe new active site configurations form and decay continuously as a result of interaction with the reactants and reaction intermediates, and maybe they even form specifically at phase boundaries arising on the evolving surface. Clearly, the only possibility we have to validate or falsify such "ideas"—and the consequences they would suggest for the design of "better" catalysts—is to study the catalyst not in UHV, not before it goes on stream, not after it has gone out of stream, but precisely *operando*, when it is working under technologically relevant gas-phase conditions.

This has exactly been the motivation of the aforementioned in situ studies on model catalysts that have made their fulminant appearance over the last decade or so [8, 9]. At spatial and temporal resolution that is ever increasing and at pressures that come closer and closer to technological conditions, such studies precisely focus on the surface structure, composition and morphology—and try to relate it to the catalytic activity. Aiming e.g. to extend the use of UHV electron spectroscopies to these pressure regimes, the experimental setups are necessarily involved. Mass flow limitations in the resulting complex reactor chambers together with still limited resolving powers render the measured data not always straightforward to interpret

[16–18]. As in many areas of materials and chemical science much synergy has therefore been achieved by complementing these measurements with modern computational theory. To a large degree these are the same (typically first-principles based) calculations of thermostability, spectroscopic signals, and reactivity descriptors as they have already been successfully conducted for a long time in the realm of UHV Surface Science. In addition, however, new theoretical approaches have been developed and advanced that have exactly the same objectives as the in situ studies [19]: For given reaction conditions in form of defined reactant partial pressures p_i and temperature T, what is the surface structure and composition—and what is the corresponding catalytic activity?

Aiming to provide this information independently, i.e. be of predictive character, such theory necessarily has to be based on first-principles electronic structure calculations. In order to account for the effect of finite temperature and pressure, as well as for the ensemble character introduced by the ongoing surface chemical reactions, these quantum mechanical calculations need to be combined with concepts from thermodynamics and statistical mechanics. Notably, two such approaches have been established that have proven so powerful that they are nowadays firmly anchored in the conceptual toolbox of everybody working in surface catalysis: (constrained) ab initio thermodynamics and first-principles microkinetics. The prior technique provides exclusively access to the surface structure and composition as a function of (T, p_i). The theory is approximate, but therefore computationally less intense and applicable to more complex surface structures. As the name implies, first-principles microkinetics explicitly accounts for the kinetic effects due to the ongoing chemical reactions. It is therefore intrinsically more accurate and additionally gives access to the catalytic activity. This comes at the price of larger computational cost and, at least in its most rigorous implementations, presently still with quite some restrictions with respect to the complexity of the surface structures and reaction networks it can handle. In this topical review I will survey both techniques, yet not so much in terms of their detailed methodological foundations and technical implementations. Extended reviews are available for this [19–22]. Instead, I will focus on their concepts, discuss some current frontiers and ongoing developments, and specifically illustrate the type of insights they provide in the context of in situ model catalyst studies.

7.2 (Constrained) Ab Initio Thermodynamics

7.2.1 Methodology

Even though they form the basis of both techniques that will be covered I will not at all dwell on the underlying first-principles electronic structure calculations [23]. In the context of in situ studies on model catalysts these calculations are at present almost exclusively performed within density-functional theory (DFT). The central output of these calculations that enters into the first-principles thermodynamics or

statistical mechanics approaches is the total energy E^{tot}, i.e. the energy contained in the chemical bonds for a defined structural configuration of atoms. For the present purposes there are two aspects of these total energies that need to be highlighted: First, the total energies are only approximate, which is primarily due to the approximate exchange-correlation (xc) functional that is employed in the DFT calculations [24]. In fact, due to the typically rather large system sizes, computationally less demanding, so-called lower-rung xc functionals are predominantly applied [19, 25, 26]. For metal catalysts these are largely still semi-local generalized gradient approximation (GGA) functionals, while for materials with more localized bonding aspects like oxides these are increasingly hybrid functionals. What this implies is that we have to expect an uncertainty in central quantities like binding energies (suitable differences of total energies) or reaction barriers (difference of binding energies at initial and transition state) that is of the order of ∼0.3 eV (∼30 kJ/mol). Of course, since we lack the exact xc functional this is only a rough estimate, and for reaction barriers some error cancelation when taking a difference from differences might make the uncertainty a bit smaller. Notwithstanding, the latter is more a hope than something to rely on. In any case, we thus have to count with potential errors that are much larger than $k_B T$. This obviously has to be kept in mind when attempting to make statements about temperature-dependent properties or even more so about catalytic activities where reaction barriers enter through exponential Boltzmann-type factors.

The other aspect to highlight is to repeat that $E^{\mathrm{tot}} = E^{\mathrm{tot}}(N_i, N_j)$, where N_i and N_j are the number of species i and j in the particular configuration that has been calculated. I distinguish here and in the following between species i that are also present in the gas phase (i.e. contained in the reactants), and species j that are not (i.e. that are only present on the solid catalyst). A straightforward comparison of the stability of two configurations on the basis of DFT total energies is therefore only possible, if both configurations contain exactly the same numbers $N'_i = N_i$ and $N'_j = N_j$ of all species i and j in the system. On the contrary, in the context of near-ambient catalysis the surface composition is precisely one of the targeted quantities, i.e. one does a priori not know how many atoms of which kind there are in the surface fringe. As already pointed out before, to the very least one would expect surface coverages of reaction intermediates to change with varying pressures. In order to find out which coverage there is for given reactant partial pressures p_i, one would thus have to compare the stability of configurations with different coverages, i.e. with differing numbers N_i. This is precisely what cannot be achieved on the basis of the E^{tot} alone. In order to answer such questions one would need to know the cost of bringing the difference in species $\Delta N_i = N'_i - N_i$ and $\Delta N_j = N'_j - N_j$ between two configurations either into one of the configurations or out of the other configuration. Thermodynamically, it would thereby not matter through which particular (atomistic) mechanism this happens. The only thing that would matter is where they ultimately come from or go to.

The entire idea of ab initio thermodynamics is to provide this information by considering such reservoirs where species go to or come from, and then work within an appropriate thermodynamic framework to compare configurations with

varying numbers of species [27–35]. Since experiments and heterogeneous catalysis are generally run at defined temperatures and reactant partial pressures, the appropriate thermodynamic ensemble for this framework is the Gibbs ensemble (T, p_i). To assess the stability of a given surface configuration, a suitable quantity to evaluate is then for instance the surface free energy per surface area A,

$$\gamma(T,p_i) = \frac{1}{A}\left[G\left(T,p_i,N_i,N_j\right) - N_i\mu_i - N_j\mu_j\right], \tag{7.1}$$

where G is the Gibbs free energy of a particular surface configuration containing N_i species i and N_j species j, and μ_i and μ_j are the chemical potentials of the corresponding reservoirs of species i and j. This surface free energy represents the cost of creating the particular surface configuration by taking all of its constituent atoms out of their respective reservoirs. Calculating $\gamma(T,\ p_i)$ for a range of potential surface configurations, the one that exhibits the lowest surface free energy is this way the most stable one that (if thermodynamics is correct) should be observed in experiment.

In order to evaluate (7.1) for a given surface configuration one needs to know the chemical potentials. For any gas-phase species i, the obvious reservoir that determines this chemical potential is the gas-phase environment itself. Approximating this gas phase as an ideal gas, it is straightforward to obtain $\Delta\mu_i = \Delta\mu_i(T, p_\mathrm{i})$, where $\Delta\mu_i = \mu_i - E^{\mathrm{tot}}(i)$ and $E^{\mathrm{tot}}(i)$ is the DFT total energy of the isolated gas-phase species i. For atoms and small molecules this can even be calculated analytically [36, 37]. For others, values can be found in thermodynamic tables [38]. For the other species j that are not present in the gas phase, e.g. species constituting the actual catalyst material, alternative reservoirs need to be found. This can often be facilitated by choosing a suitable reference configuration and evaluating only the excess surface free energy with respect to this reference

$$\gamma(T,p_i) - \gamma_o(T,p_i) = \frac{1}{A}\left[G\left(T,p_i,N_i,N_j\right) - G_o\left(T,p_i,N_i',N_j'\right) - \Delta N_i\mu_i - \Delta N_j\mu_j\right], \tag{7.2}$$

where γ_o and G_o are the surface free energy and Gibbs free energy of the reference configuration, respectively. This has the advantage that one only needs to define reservoirs for non-gas-phase species j, for which $\Delta N_j \neq 0$. If we are for instance interested in evaluating the relative stability of different surface coverages of a given reactant on the surface of a solid catalyst, then the clean surface at zero reactant coverage is obviously a useful reference configuration. In this case we would only need to determine a suitable reservoir for species constituting the catalyst and not being present in the gas phase, if the changing concentration of adsorbed reactants would actually affect the density of catalyst species in the surface fringe. In the case of compound materials, such a density change could thereby for example proceed via precipitation of another (bulk) phase. In this case, this other phase, say for instance pure metal droplets at the surface of metal oxide

catalysts, is in turn a suitable reservoir defining the chemical potential of the substrate species involved in the density change.

What is thus left to get hard numbers out of (7.1) or (7.2) is to compute the solid-state Gibbs free energies (and equivalently the chemical potentials of the non-gas-phase reservoirs). Similar to the procedure for the gas-phase species, it is thereby useful to separate off the DFT total energy, which in terms of thermodynamic potentials amounts to the Helmholtz free energy minus the zero point energies. We thus have $G = E^{\mathrm{tot}} + \Delta G(T,\ p_i)$, where the zero point energies are now considered to be contained in the temperature and pressure dependent free energy part $\Delta G(T,\ p_i)$. In comparison to the ideal gas situation, calculating this free energy part is more involved for solids, and, unfortunately, the term itself is also generally not negligible [39–41]. Fortunately, however, it is not this absolute free energy part that matters for calculating in particular the excess surface free energy. As apparent from (7.2) it is only the difference of two solid-state Gibbs free energies and additional chemical potentials that enters, and in this difference many contributions can cancel. Since the predominant contribution to solid-state $\Delta G(T,\ p_i)$ comes from vibrational free energy, it is thus not the absolute vibrations that enter. Instead it is only changes of these vibrations (phonon spectrum, to be precise) with respect to the reference configuration that matter, and these changes can often be neglected for a first assessment. In the difference of (7.2)—and only there—we can then write

$$\gamma(T,p_i)-\gamma_o(T,p_i)\approx\frac{1}{A}\left[\Delta E^{\mathrm{tot}}-\Delta N_i\Delta\mu_i(T,p_i)\right] \tag{7.3}$$

with

$$\Delta E^{\mathrm{tot}}=E^{\mathrm{tot}}\left(N_i,N_j\right)-E_o^{\mathrm{tot}}\left(N_i^{'},N_j^{'}\right)-\Delta N_iE^{\mathrm{tot}}(i)-\Delta N_jE^{\mathrm{tot}}(j)$$

and $E^{\mathrm{tot}}(j)$ the DFT total energy of the solid-state reservoir chosen for species j. In this approximation, the computational demand to evaluate the excess surface free energy of a given configuration is therefore reduced to DFT calculations of the surface configuration, the reference surface configuration, as well as of all isolated gas-phase species and the chosen additional solid-state reservoirs. The entire temperature and pressure dependence is instead exclusively contained in the terms $\Delta N_i\Delta\mu_i(T,p_i)$, where $\Delta\mu_i(T,p_i)$ is a look-up quantity that is generic for the species and not for the particular systems studied.

It is this low computational demand that makes this formulation of ab initio thermodynamics so appealing. One has to stress that this holds only within this prevalent approximation though. The neglected terms $\Delta G(T,\ p_i)$ are more involved. This refers thereby less to the predominant vibrational contribution to these terms, which can be and needs to be at least approximately calculated in many cases [39, 41]. The more elusive contribution comes instead from the configurational entropy [20]. Fortunately, for not too high temperatures this entropy is not large and for

hitherto typically studied systems neglecting it affects the results only in a predictable way that I will further discuss below.

There is, however, a much more critical aspect than the neglect of these individual solid-state free-energy contributions. This is the way how the configurational sampling is performed in present applications of this theory. What is generally done is to consider a given number of configurations that is presumed to be of relevance for the problem at hand. Computing the excess surface free energies for every one of them, one of these configurations will exhibit the lowest value for given gas-phase conditions (T, p_i). This configuration is then declared to be most stable for these conditions, but obviously this statement can only refer to relative stability within the group of configurations that has actually been tested. If a configuration that was not considered was to exhibit an even lower excess surface free energy, it would not be identified. There is also no warning mechanism of such cases in any form in the present formulation of ab initio thermodynamics: The results obtained would simply be wrong. This limitation with respect to the considered configurations must always be born in mind when assessing the results of present-day ab initio thermodynamics studies. Of course, this limitation is not conceptual, but results merely from the steeply increasing computational costs when comparing extended numbers of configurations (certainly in the context of in situ studies of model catalysts). Any form of more systematic configurational sampling, as e.g. resulting from global geometry optimization algorithms, can be straightforwardly incorporated into the ab initio thermodynamics framework. The resulting total energies of all configurations sampled just need to be entered into thermodynamic equations of the type of equations (7.1)–(7.3), or one directly performs the sampling in the appropriate thermodynamic ensemble by evaluating different cost functions than the total energy.

7.2.2 Oxide Formation at (Near-)Ambient Conditions

After this brief methodological survey, let me illustrate the kind of insights and the effect of the discussed approximations and limitations with an application example in the in situ context. As mentioned before, a possible formation of oxides at the surface of late transition metal oxidation catalysts is a prototypical manifestation of the type of surface morphological transitions that one suspects to occur under technologically relevant, (near-)ambient reaction conditions. While nominally Rh, Pd, or Pt would thus be materials that one cites as catalysts employed for such reactions, in fact their oxides or "oxidic" films could be the ones that really actuate the catalysis. If true, it would obviously not make much sense to discuss the catalytic activity (and any "ideas" for improved catalysts) in terms of the classic active sites offered by fcc(111) of fcc(100) facets of these metals. One would have simply looked at the wrong material. Ab initio thermodynamics has been heavily employed in this context and a natural starting point is to only consider the effect of an oxygen environment. Using the clean metal surface as a suitable reference, one

would calculate the excess surface free energy for a range of surface configurations with increasing oxygen content, and in turn evaluate their relative stabilities as a function of the oxygen chemical potential of the surrounding gas phase. Figure 7.1 exemplifies this for a Pd(100) surface [42–44]. Natural surface configurations to consider in such a case are various (ordered) simple adsorption layers of different concentrations as they could for example have been characterized in UHV Surface Science work. For the O/Pd(100) surface this would be so-called $p(2 \times 2)$ and $c(2 \times 2)$ structures with O atoms adsorbed at the fcc(100) hollow sites at ¼ monolayer (ML) and ½ ML coverage, respectively [45, 46]. The excess surface free energies of these structures will vary with varying O content in the gas phase. In (7.3) this enters through the linear dependence on the (oxygen) chemical potential, which scales differently for configurations with different amounts of (oxygen) species incorporated into the surface fringe. In the limit of an infinitely dilute gas ($\Delta\mu_O \rightarrow -\infty$), incorporating any O into the surface configuration would incur an infinite cost due to the concomitant infinite loss of entropy. This is why the clean surface reference naturally exhibits the lowest excess surface free energy under these conditions, cf. Fig. 7.1a.

With increasing oxygen content in the gas phase, $\Delta\mu_O$ will become less negative and it will become increasingly more favorable to stabilize oxygen at the surface. In

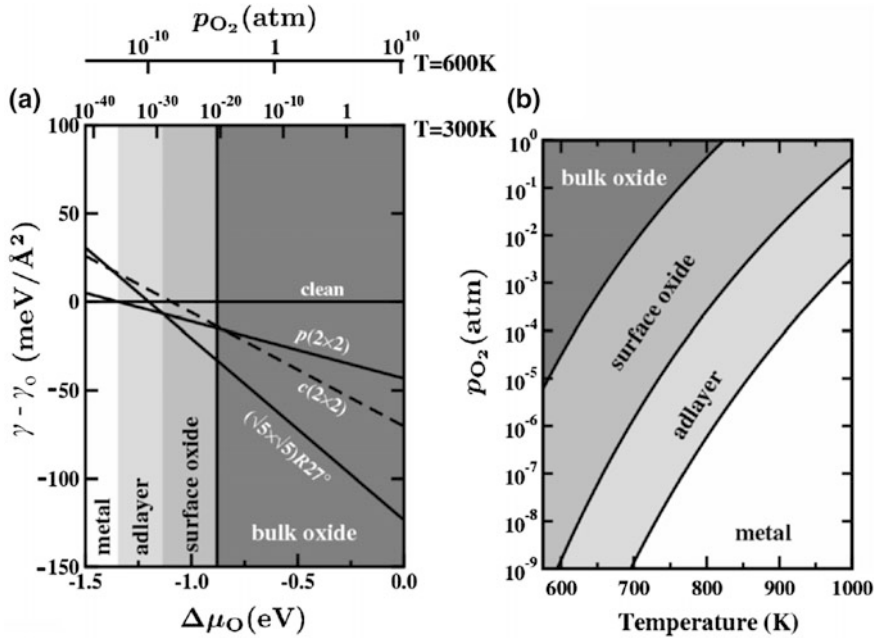

Fig. 7.1 **a** Excess surface free energies and **b** surface phase diagram for O/Pd(100). Considered are two ordered O adsorbate layers with different coverage ($p(2 \times 2)$, ¼ monolayer (ML), and $c(2 \times 2)$, ½ ML) and a ($\sqrt{5} \times \sqrt{5}$)R27°–O surface oxide film (0.8 ML). Note the extended stability range of the surface oxide compared to the known PdO bulk oxide. The total energies (DFT-GGA, PBE) used to construct this graph via (7.3) are taken from [42–44]

the example of O/Pd(100) in Fig. 7.1a this happens at $\Delta\mu_O = -1.3$ eV, which is when the excess surface free energy of the $p(2 \times 2)$ adsorption structure becomes lower than the clean surface reference. The higher the surface O concentration of a configuration, the steeper will be the decrease of its excess surface free energy in a plot like Fig. 7.1a. This can eventually stabilize such configurations at higher O chemical potentials. The obvious upper limit of surface O concentration is thereby a complete transformation of the bulk metal into a bulk oxide, as this then implies an infinite number of O atoms in the normalization per surface area employed in (7.3) [47]. In a plot like Fig. 7.1a this leads to an infinite negative slope, i.e. a vertical excess surface free energy line. For the shown example of O/Pd(100) this line indicating the formation of bulk PdO lies at $\Delta\mu_O = -0.7$ eV, and for any higher oxygen chemical potential the PdO bulk oxide will be the stable phase.

Already at this stage it is worthwhile to point out what has been gained through this theory. On the basis of only a handful of static DFT calculations we can discuss the possible surface structure and composition at finite temperature and pressure. In a plot like Fig. 7.1a the latter two-dimensional (T, p_{O2})-dependence is thereby conveniently described through the one-dimensional dependence on the corresponding chemical potential. By defining suitable references one can convert one dependence into the other on an absolute scale [34]. As done in Fig. 7.1a this allows to include additional x-axes that give the pressure dependence at some specific temperature (or alternatively the temperature dependence at some fixed pressure). The surface configuration exhibiting the lowest excess surface free energy for a certain range of chemical potentials would be identified as the most stable one for the corresponding gas-phase conditions. Another way of plotting the results would be to concentrate only on these most stable structures and plot their (T, p_{O2})-stability ranges in a so-called surface phase diagram as done in Fig. 7.1b. Such surface phase diagrams are more intuitive to read, but there is also a certain *caveat* to them. This has to do with the uncertainty due to the mentioned approximate DFT total energies. For a surface phase diagram this implies that the obtained boundaries between different phases can typically be wrong by ~100 K and (depending on temperature) several orders of magnitude in pressure. As a large part of the error arises often from the DFT description of the gas-phase species, such shifts tend to similarly apply to all phase boundaries though. The overall topology of the surface phase diagram (which phases are predicted to be stable at some finite range of (T, p_{O2})-conditions) is then more robust, and this is what one should generally focus on. In this respect, an intriguing immediate result contained in the O/Pd(100) example of Fig. 7.1 is for example that the $c(2 \times 2)$ adsorbate structure which has been observed and characterized after gas dosage in UHV [45, 46] is never predicted to be a stable phase on the basis of the employed DFT functional.

A second intriguing aspect of ab initio thermodynamics that can be highlighted with the example of Fig. 7.1 is the possibility to test the stability of surface configurations one suspects to potentially play a role at finite temperatures and pressures. In the context of oxide formation this would prominently be thin oxide films at the surface. For O/Pd(100) such a structure had again be stabilized after excessive O dosage in UHV and was subsequently characterized as a layer of PdO(101) in a

commensurate ($\sqrt{5}$ x $\sqrt{5}$)R27° stacking on top of Pd(100) [48, 49]. Evaluating the excess surface free energy for this surface structure, there is indeed a finite range of O chemical potentials where it is predicted to be most stable, cf. Figure 7.1. This range extends over $\Delta\mu_O$ lower than the ones of the known bulk oxide phase, i.e. ab initio thermodynamics predicts a range of less O-rich gas-phase conditions where bulk PdO is not yet stable, but such a PdO(101) overlayer is. Such an extended stability range of surface oxide films has been found for many low-index late transition metal facets [48–57]. It can arise from an enhanced coupling of the film to the underlying metal [58], but also simply because the structure of the thin films is by no means restricted to those of the known bulk oxides. The latter point thereby hints at the mentioned limitation of prevalent ab initio thermodynamics with respect to the configurational sampling. Maybe there are more complex, highly O-enriched surface configurations that would exhibit even lower excess surface free energies. Without knowing their explicit structure (or being able to represent this structure in computationally tractable periodic supercell geometries) their excess surface free energies cannot be calculated and the corresponding stabilities not be assessed. Even within the drive towards (near-)ambient catalysis this underscores the value of dedicated UHV Surface Science work that aims to stabilize and characterize such structures and therewith serves as a generator for structural models to test. Just as much as one might rather focus more on the overall topology of surface phase diagrams than their absolute phase boundaries, this also suggests that the really valuable "idea" that has emerged out of studies of the kind of the discussed O/Pd(100) work is not necessarily that of a particular, defined surface oxide structure. These ordered structures are likely just idealized models. Instead it is the general notion that such kind of O-enriched surface configurations (be they called surface oxides, oxidic films or sub-surface oxygen) can be stabilized in environments far less O-rich than those where bulk oxides are known to be stable.

7.2.3 *Constrained Thermodynamics: Approximate Structure and Composition Under Reaction Conditions*

Whether such configurations really play a role for (near-)ambient oxidation catalysis, then critically depends on the particular reaction. The presence of the other reactant tends to reduce the catalyst surface. In order to assess whether an oxidized configuration will prevail under reactive conditions, the other reactant thus needs to be accounted for. In ab initio thermodynamics this seems straightforward to do as a multi-component gas phase can simply be considered through multiple reservoirs for the corresponding gas-phase species [39]. In (7.1)–(7.3) this is already indicated through the dependence on several chemical potentials μ_i. There is a slight catch to this for heterogeneous catalysis though. If one was to consider full thermodynamic equilibrium, then also these various reservoirs would be in equilibrium with each other. However, if all reactants were in full equilibrium with each other, the gas phase would only consist of products, as a catalyst can only operate under

gas-phase conditions where the products are thermodynamically more favorable than the reactants. As this is obviously not the situation we want to describe, one instead suitably resorts to a kind of "constrained" equilibrium approach [37, 59]. In order to capture the effect of exposure to the reactant gas phase, the catalyst surface is considered to be in full equilibrium with all reactant gas-phase chemical potentials, while the latter are treated as mutually independent of each other. The approximation that is introduced through this is to neglect that the actual on-going surface catalytic reactions may consume surface reaction intermediates faster than they can be replenished from the gas phase [60]. A "constrained" ab initio thermodynamics study can therefore only provide some first rough insight into the surface structure and composition in reactive environments, but its advantage is that, as before, a wide range of structurally and compositionally largely differing configurations can readily be compared in a computationally undemanding way.

Figure 7.2 illustrates this for the CO oxidation at Pd(100) system, where in contrast to Fig. 7.1 the CO chemical potential is now explicitly considered as a second axis [43, 44]. Comparing the stability of a large set of on-surface (co) adsorption, surface oxide and bulk oxide structures, several phases involving the $(\sqrt{5} \times \sqrt{5})R27°$ surface oxide are found to be most stable over a wide range of (T, p_{O2}, p_{CO})-conditions. Again, this range largely exceeds the stability range of bulk PdO. Intriguingly, this range extends in fact so much that it even just touches the gas-phase conditions typical for technological CO oxidation, i.e., partial pressures of the order of 1 atm and temperatures around 300–600 K. In terms of a potential oxide formation under reaction conditions, this would suggest that instead of thick bulk-like oxide films it would rather be such a nanometer-thin oxidic overlayer that could play a role. Indeed, in situ reactor scanning tunneling microscopy (STM) experiments observed substantial morphology changes that were precisely assigned to the formation of a thin oxidic overlayer [56, 61, 62]. However, in these experiments, a continuous consumption and formation of this surface oxide even under the employed steady-state reaction conditions was reported—which would directly relate to the general "idea" of a working catalyst as a very dynamic entity. For this aspect the proximity of the technologically-relevant (near-)ambient reaction conditions to the phase boundary between the surface oxide and reduced metal configurations in Fig. 7.2 has to be emphasized. In Fig. 7.2 this boundary is drawn as an infinitely sharp transition, whereas in reality any such phase transition would occur over a finite range of pressures and/or temperatures. This abrupt change in (μ_O, μ_{CO})-space in Fig. 7.2 is the result of the neglect of the solid-state configurational entropy contributions in (7.3). While these contributions are generally small compared to absolute excess surface free energies, they particularly matter for chemical potential conditions where the excess surface free energy lines of two competing configurations cross, i.e. exactly at phase boundaries. Under such conditions the thermally induced possibility to explore both configurations leads to enhanced fluctuations and phase coexistence [37, 59].

Under the neglect of configurational entropic contributions the prevalent formulation of (constrained) ab initio thermodynamics cannot explicitly account for such a phase coexistence (and the implied fluctuations). As done in Fig. 7.3 one

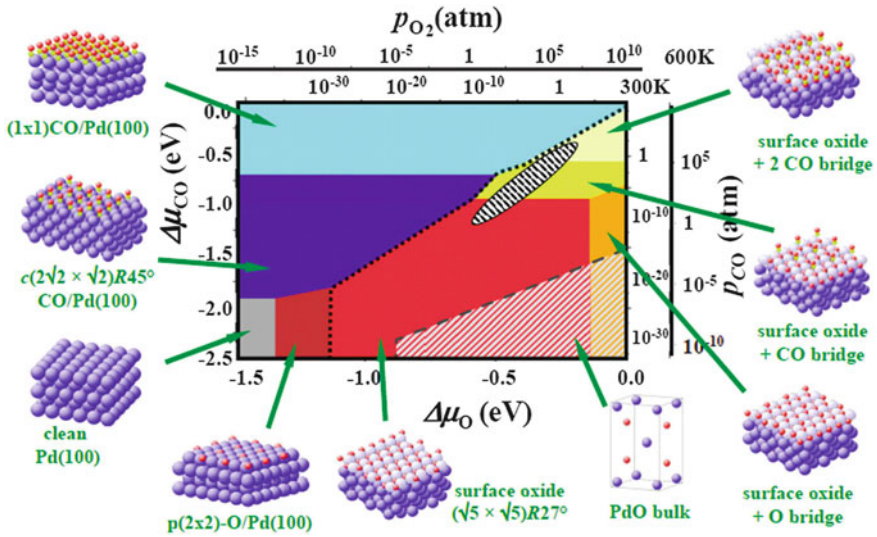

Fig. 7.2 Surface phase diagram for the Pd(100) surface in "constrained" thermodynamic equilibrium with an environment consisting of O_2 and CO. The atomic structures underlying the various stable (co-)adsorption phases on Pd(100) and the $(\sqrt{5} \times \sqrt{5})$R27° surface oxide, as well as a thick bulk-like oxide film (indicated by the bulk unit-cell), are also shown (Pd: large blue spheres, O: small red spheres, C: white spheres). Phases involving surface or bulk oxide are to the right bottom of the dotted and dashed line, respectively. The dependence on the chemical potentials of O_2 and CO in the gas phase is translated into pressure scales at 300 and 600 K. The black hatched ellipse marks gas-phase conditions representative of technological CO oxidation catalysis, i.e., partial pressures of 1 atm and temperatures between 300 and 600 K. Adapted from [43]

may estimate its width in (T, p_i)-space and represent this information by drawing the phase boundaries as regions with a corresponding finite width [37, 59]. Figure 7.3 shows results equivalent to Fig. 7.2, but obtained for CO oxidation at RuO_2(110) [60]. Strikingly, technologically relevant feed conditions fall again precisely into such a phase coexistence region. The thus suggested notion to view heterogeneous catalysis as a phase transition phenomenon may thereby be rationalized by recalling that a so-called stable phase is not stable on an atomistic scale. Instead it represents an average over many continuously on-going processes such as dissociation, adsorption, diffusion, association, and desorption. As all these elementary processes and their interplay are of crucial importance for catalysis, regions in (T, p_i)-space that exhibit enhanced thermal fluctuations, i.e. where the dynamics of these atomistic processes is particularly strong, appear naturally as most relevant [37]. In this understanding where in phase space catalytically relevant regions might emerge, insights of the type provided by Figs. 7.2 and 7.3 also allow to comment on the possibility to further explore them by bridging the pressure gap between (near-)ambient real catalysis and UHV Surface Science. In the thermodynamic Gibbs ensemble the only ruling quantities are the chemical potentials μ_i.

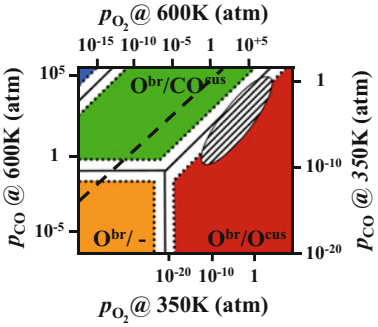

Fig. 7.3 Surface phase diagram for the $RuO_2(110)$ surface in "constrained" thermodynamic equilibrium with an environment consisting of O_2 and CO. The labels of the different stable phases reflect a predominant population (O, CO or empty "–") of the two prominent adsorption sites offered by this surface, br(idge) and coordinatively unsaturated (cus) site. Coexistence regions at the phase boundaries are marked in *white*, with the width of these regions corresponding to 600 K. Technologically relevant catalytic conditions around partial pressures of 1 atm and temperatures between 300 and 600 K are indicated by the *black* hatched ellipse. Above the *dashed line* bulk RuO_2 is thermodynamically unstable against CO-induced decomposition (see text). Adapted from [60]

As long as the (T, p_i)-conditions of two experiments correspond to the same μ_i, thermodynamically the same results would be expected. In order to represent the chemical potentials of (near-)ambient catalysis in UHV Surface Science one would correspondingly have to resort to much lower temperatures, cf. the different pressure scales in Figs. 7.2 and 7.3. Note, however, that this idea of thermodynamic scaling by maintaining the same chemical potentials is not necessarily the same as simply maintaining a constant reactant partial pressure ratio and varying the total pressures or temperature. Such a procedure does not keep the chemical potentials constant, and in case of dissociatively adsorbing reactants generally not even the chemical potential ratios. Without knowledge of the surface phase diagram, the concomitantly explored chemical potential range may easily cross phase boundaries, and then lead to incomparable results even on thermodynamic grounds alone.

Obviously, also kinetic limitations will contribute to deviations from thermodynamic scaling and further jeopardize a reliable bridging of the pressure gap by simple thermodynamic recipes for the gas-phase concentrations [10]. Such kinetic effects are thereby not necessarily more prominent at low temperatures. At higher temperatures one may generally expect higher turnover frequencies. The surface-reaction processes might thus increasingly occur at higher rates than the adsorption and desorption processes that maintain the equilibrium with the surrounding gas phase that is assumed in (constrained) ab initio thermodynamics. As further discussed below, the resulting depletion of particular surface species may then well lead to significant deviations from the predicted surface structure and composition [60]. Already for the pure formation of the thin surface oxide overlayer on Pd(100) at increasing O pressures, in situ surface X-ray diffraction (SXRD) experiments indicated severe kinetic limitations that suppressed formation of the overlayer at near-ambient pressures and elevated temperatures

on the time scale of hours [42]. One may well imagine such limitations to intensify in the presence of a reducing co-reactant, or when formation of thick bulk-like films is concerned. This should be kept in mind when assessing the results of Fig. 7.3. For the more reactive Ru metal, the stability region of its bulk RuO_2 oxide is much larger than for Pd and PdO [47]. In terms of the surface phase diagram, technologically-relevant reaction conditions fall therefore well into the stability region of this bulk oxide, cf. Fig. 7.3. Instead of a potential (dynamic) formation of a nanometer-thin surface oxide overlayer as on Pd(100), this would rather suggest thick bulk-like oxide films to occur on Ru, with the catalytic phase coexistence then restricted to the adsorbate overlayer on these films. However, kinetic growth limitations, e.g. due to slow diffusion of either O or Ru atoms through the formed film [63, 64] might significantly change this picture. Indeed, while the formation of crystalline, bulk-like RuO_2(110) during (near-)ambient CO oxidation catalysis has indeed been observed experimentally at Ru(0001), even after long operation times the reported film thicknesses never exceeded about 20 Å [13, 65, 66].

This restates to really view the results of (constrained) ab initio thermodynamics only as very rough first insights. However, even on this level these insights can be very valuable and in the discussed context of oxide formation in (near-)ambient oxidation catalysis these insights do support the dynamical catalysis picture in terms of substantial surface morphological transformations in the reactive environment that has emerged from corresponding in situ experiments. In fact, as there is no reason why a possible formation of (surface) oxides should simultaneously occur on different facets of the same metal, such transformations can also contribute to substantial changes in the shape and morphology of (supported) nanoparticles. (Constrained) ab initio thermodynamics can also contribute to this context by calculating surface free energies of different facets and combining them within Wulff (Kaischew) constructions [67, 68]. Significant particle shape changes have this way indeed been predicted as a function of the surrounding gas-phase environment [69–72]. The possibility to quickly compare surface configurations that vary as widely as metal, oxidic overlayer, and bulk-like oxides is thereby an asset that—behold of the highly approximate nature of this theory—cannot be overstated and that serves ideally to elucidate the dynamics of working catalysts.

7.3 First-Principles Microkinetics

7.3.1 Methodology

In order to properly capture the kinetic effects that are suspected to modify the approximate picture obtained within ab initio thermodynamics, the simulations need to explicitly account for a time dependence. The involved time integration is thereby extensive and may exceed time scales of the order of seconds. The reason for this is the so-called rare-event dynamics underlying surface catalytic processes.

While a catalyst generally reduces the barriers of these processes, they are still typically of the order of ~1 eV. Since this is much larger than $k_B T$, the time scales of these relevant elementary processes are largely decoupled from the regular thermal (vibrational) motion. A vanilla-flavor molecular dynamics simulation integrating the Newtonian equations of motion for the nuclei would be able to capture these vibrations. Yet, it is largely intractable to integrate up over time scales that would allow for a statistically relevant averaging of the rare catalytic processes.

In microkinetic theories this separation of time scales is instead exploited by abandoning the continuous dynamical description in favor of a discrete state-to-state time evolution, in which the individual elementary processes drive the system in discrete jumps from one system state to the next [73, 74]. The central equation to solve is then a Markovian master equation

$$\frac{dP_\alpha(t)}{dt} = \sum_\beta \left[W_{\alpha\beta} P_\beta(t) - W_{\beta\alpha} P_\alpha(t) \right], \tag{7.4}$$

where α and β are states of the system with corresponding probabilities $P_\alpha(t)$ and $P_\beta(t)$. $W_{\alpha\beta}$ and $W_{\beta\alpha}$ are the transition probabilities per unit time, specifying the rate with which the system changes due to the elementary processes (adsorption, desorption, reaction, and diffusion), respectively from state β to α and vice versa. These master equations, one for each system state α, are thus simple balancing equations: The probability to find the system $P_\alpha(t)$ in state α at any time t changes because transitions from any other state β can occur into state α ($W_{\alpha\beta} P_\beta(t)$) or they can occur out of state α into any other state β ($-W_{\beta\alpha} P_\alpha(t)$). Importantly, one has thereby applied a Markov approximation, because none of these transitions depend on the history through which states the system has gone before. Rather than involving probabilities that depend on any past time $t' < t$, (7.4) thus only shows probabilities at the same instant in time t: Transitions involving a hopping out of state α at time t depend only on the probability that the system actually is in state α at time t ($P_\alpha(t)$). Transitions involving a hopping from any other state β into state α at time t depend only on the probability that the system is in state β at this time ($P_\beta(t)$). The rationale behind this approximation is that one assumes that during the long vibrational motion before a rare event eventually brings the system out of the current state into the next one, the system completely forgets how it actually got into this state in the first place. Limitations in the dissipation of the reaction energy released during individual elementary processes might potentially lead to violations of this Markov approximation [15], but for the time being this approximation is unanimously assumed in prevalent formulations of chemical kinetics.

For a small number of system states, a Markovian master equation like (7.4) can be solved analytically. Unfortunately, in surface catalysis we are not facing such a small number. On the contrary. Assume that our catalyst surface exhibits a total of N active sites. A unique system state would then be defined by the detailed population of every single one of these sites, and any elementary process that changes the population of one or more of these sites corresponds to one entry in the

transition matrix $W_{\alpha\beta}$ [75]. Since the examples I use are for CO oxidation catalysis, let's stick to this reaction to see what this means in terms of numbers. In this reaction, any active site can either be empty, or occupied by the reaction intermediates O or CO (if we assume that CO_2 formation leads to immediate desorption of the product). This yields three population possibilities for every site and if we for example assume that there are $N = 100$ active sites, then the total number of system states, also known as detailed population configurations of the sites, is $3^{100} \approx 10^{47}$. Obviously, this is not a small number and for any more complex reaction network with a correspondingly increased number of different reaction intermediates it will even be higher. Yet, we still have to rationalize why $N = 100$ should be a good representation for an extended catalyst surface. This comes about as in order to appropriately capture the ensemble effects at such a surface, the explicitly considered group of active sites (that is suitably continued through periodic boundary conditions) must be large enough to exceed the correlation length between sites. This is the length over which the statistics of the processes that are ongoing at one site still influences the statistics of the processes that occur at another. From present experience on the type of systems discussed in this review an area spanned by $(10 \times 10) = 100$ sites is a good (in fact lower) estimate for this [22, 75].

For a surface catalytic system we thus have to generally expect a transition matrix with a dimension of the order of $\sim(3^{100} \times 3^{100})$ or larger, i.e. with at least $\sim(3^{100})^2 \approx 10^{95}$ matrix elements. Fortunately, most of these matrix entries are zero [75]. This has to do with the fact that chemical elementary processes typically affect only the population of a small number of sites. A unimolecular adsorption or desorption event of a molecule like CO changes the occupation of one particular site. A diffusion process of such a molecule changes the occupation at two active sites, one being emptied and an empty one being filled. Any transition connecting states that differ in their populations by more than a few individual sites has therefore a $W_{\alpha\beta} = 0$. An additional important feature that simplifies the transition matrix immensely is translational symmetry at a crystalline extended surface. In such a situation our ensemble of $N = 100$ active sites may only comprise a much smaller number of inequivalent site types. At a simple low-index metal surface maybe something on the order of two or three, say hollow or bridge terrace sites or high-symmetry sites at an upper or lower step edge. In the crystalline symmetry the elementary processes occurring at any site type are equivalent, which means that their corresponding transition matrix elements $W_{\alpha\beta}$ are the same. While the total number of non-zero matrix elements even in the largely sparse transition matrix is thus generally still too large to even be stored, the total number of inequivalent matrix entries $W_{\alpha\beta}$ is then typically rather small and determined by the total number of inequivalent elementary reactions in the reaction network [75–77]. For a simple CO oxidation model comprising only one active site type this total number can in fact be as low as seven: Dissociative adsorption of O_2, associative desorption of two adsorbed O, CO adsorption, CO desorption, O diffusion, CO diffusion, and CO + O reaction. It is only this immense simplification due to a prevailing and despite the ongoing catalytic reactions static crystalline symmetry that makes any kind of microkinetic model computationally tractable today. I come back to this point later,

but already here we should realize that this obviously clashes with our working hypothesis of a dynamically evolving, possibly amorphous or highly heterogeneous catalyst surface that we intend to scrutinize with such simulations. This is precisely the dilemma. We are largely constrained to conduct microkinetic simulations within static models focusing on impinging and reacting gas-phase species on a rigid solid surface. In a self-fulfilling prophecy this then contributes to the present widespread acceptance of such a picture of catalysis.

Even though the transition matrix is thus sparse and contains only few non-equivalent non-zero matrix elements, this does not change the fact that its dimension is of the order of $\sim(3^{100} \times 3^{100})$ already for the discussed CO oxidation reaction. While in the notation of (7.4) the master equation has a deceptively simple form, it is hence so high-dimensional that it generally escapes any direct solution. Kinetic Monte Carlo (kMC) simulations overcome this problem by generating an ensemble of state-to-state trajectories with the property that an average over the entire ensemble of trajectories yields the probability densities $P_\alpha(t)$ of (7.4) [21, 22]. In this way, only those matrix elements $W_{\alpha\beta}$ of transitions between states α and β are required that are actually executed along the generated trajectories. Despite the averaging over the trajectory ensemble, a central feature of the finally obtained explicit numerical solution is thereby that it contains the information of the detailed spatial distribution of the reaction intermediates over the considered active sites, along with the equally resolved occurrence of the individual elementary processes. The still prevailing alternative to achieve a solution of (7.4) discards this detailed information and instead considers only the occupation probabilities at different site types, i.e. the averaged coverage θ of all equivalent sites of a given type [5–7]. This represents a significant simplification of the problem, as the master equation then decays into a small number of differential rate equations describing the time evolution of these coverages at the different site types [78, 79]. These are exactly the type of rate equations that are often phenomenologically formulated. Typically the resulting network of differential equations is extremely stiff and requires special solution techniques. Nevertheless, even then the computational solution is so undemanding that it can mostly be achieved on time scales of the order of seconds on simple desktop computers.

There is also an additional simplification with respect to the input that such a mean-field (MF) rate equation model requires. It only needs to know what kind of active site types are considered and which elementary processes can take place at each one of them. In contrast, as it resolves the spatial distributions at the surface, a kMC model additionally needs to know how these active site types are geometrically arranged with respect to each other. As already mentioned such simulations are presently only tractable under a prevailing translational symmetry. Typically, kMC simulations in the field are therefore performed for a given lattice model that reflects the crystalline structure of the studied single crystal surface or nanoparticle facet. From this perspective, and recalling our objective to investigate a possible dynamical picture of catalysis, this sounds like a disadvantage or limitation in comparison to the MF rate equation approach. To some extent this is true. On the other hand, one has to realize that an MF model does not even know whether there

is a crystalline order at the surface or not. It does not even know that step sites are per definition linearly coordinated next to each other and are thus differently accessible to surface reaction intermediates than active sites at a two-dimensional terrace. The only thing an MF model knows and can correspondingly account for is that there are the different active site types that it considers. Obviously, MF rate equation theory is thus a gross approximation in comparison to kMC and we can only expect it to yield a faithful description of the surface kinetics if this approximation is justified. The latter is the case, when there is a perfect mixing of the reaction intermediates over the active sites of the surface. Then, indeed, the details of the spatial distribution do not matter. Fast diffusion processes can ensure such a mixing. In turn, diffusion limitations, as we can often expect them for example at oxide surfaces, are one of the two classic situations known to cause a break-down of the MF approximation, with rate equation theory correspondingly providing inaccurate solutions [79, 80]. The other situation arises in the case of strong lateral interactions between reaction intermediates, as the implied preferences of certain reaction intermediates to either seek or avoid each other naturally oppose the diffusional tendency to randomly mix the adlayer [78]. As it is not a priori obvious if the MF assumptions are fulfilled for a given system, MF rate equation theory should not be applied uncritically. Clearly, if they are fulfilled, MF theory is the much more efficient approach that should be pursued. If they are not fulfilled, wrong results and concomitant "ideas" might result.

KMC and MF rate equations are presently the two predominant microkinetic theories. As rate equations are the far more traditional and widespread approach, people often exclusively associate them with the label microkinetic modeling. This is sloppy as both theories formally provide solutions to the same microkinetic master equation. With the rapidly advancing use of kMC simulations in the field of surface catalysis one should thus rather refer to microkinetic modeling as a joint label for both approaches. The formal similarity of the two approaches is also reflected in the equivalent input they require. As already discussed these are the inequivalent active sites (in kMC additionally a lattice model fixing their geometrical arrangement) and the list of elementary processes that can occur at these sites. It is worthwhile to emphasize that this is an input, not an outcome of the simulations. Neither approach has any built-in warning feature if a relevant process or site type has been overlooked, or even more desirable the capability to automatically generate complete lists of such processes and sites. If a relevant process or site is not included in the microkinetic model, the results are nothing, but simply just wrong.

7.3.2 The First-Principles Input

Apart from these lists the remaining input that is additionally needed are the inequivalent, non-zero transition matrix elements. With units of time^{-1}, these matrix elements correspond to the rate constants of the various elementary

processes, i.e. $W_{\alpha\beta} = k_a$ if the transition from state α to state β results from elementary process a with rate constant k_a [22, 75]. In first-principles (1p) microkinetic approaches these rate constants are determined by electronic structure theory calculations, and it is through these rate constants that such kind of modeling then obtains its (hopefully) predictive character. To derive the rate constants predominantly from computationally less demanding static, again typically DFT, calculations, the currently most commonly employed approach in the area of surface catalysis is transition-state theory (TST) [19, 81, 82]. Without having seen much systematic scrutiny, this approach seems to meet sufficient accuracy, which is thus quite different to the situation in other fields e.g. when liquids are involved. TST yields rate constants of a general form

$$k_a = A(T, p_i)\exp\left(\frac{-\Delta E_a}{k_B T}\right), \tag{7.5}$$

where the prefactor $A(T, p_i)$ accounts for entropic changes between the initial and transition state (TS) of the process, and ΔE_a is the corresponding energy barrier. As the prefactor enters this equation only linearly, various, in parts drastic, approximations for it characterize the present state-of-the-art in the field [19, 83]. In particular for adsorption or desorption processes or Eley-Rideal reaction steps that may involve large entropy changes this will have to be improved in future work [60, 84]. Apart from their direct quantitative impact on the rate constant and subsequently the microkinetic simulation result, such approximations have generally also to be seen in the light of microscopic reversibility. In order to be thermodynamically consistent, rate constants of forward and (time-reversed) backward processes like adsorption and desorption have to fulfill a detailed balance condition. If different approximations are made for the two processes, this condition can be broken. Kinetic models that correspondingly do not yield the proper thermodynamic limits should be met with great skepticism, but are unfortunately frequently found in the literature.

This leaves as most crucial DFT input the energy barriers ΔE_a for every inequivalent elementary process a. Already for decently sized reaction networks and considering only a few inequivalent active site types, the explicit calculation of these barriers quickly becomes the predominant computational bottleneck of 1p microkinetic studies [19]. This in particular, as the ΔE_a generally depend on the local environment, i.e. lateral interactions with nearby co-adsorbates modify the energy barriers. In order to capture such effects, multiple DFT calculations of the same process need to be performed for different local adsorbate configurations. In 1p-kMC simulations these are then cast into some (short-range truncated) lattice-gas Hamiltonian expansion [85–88], while in 1p-MF rate equation theory this dependence is considered through an effective coverage-dependence $\Delta E_a = \Delta E_a(\theta)$ [7, 89, 90]. In their prevalent formulation 1p microkinetic studies thus carry an enormous overhead. Extensive DFT calculations are required to determine all process barriers and their environment dependencies. This information is then stored in look-up tables, which serve as basis for the subsequent and

computationally typically far less demanding actual 1p-kMC or 1p-MF rate equation simulations. An obvious disadvantage of such a static divide-and-conquer type procedure is that potentially extensive DFT calculations are performed for reaction intermediates or coverage regimes that in the actual microkinetic simulations for the targeted reaction conditions are never met.

A pragmatic solution to this is to start with quite simple formulations for the reaction network and lateral dependencies, possibly using lower-level theories for an only approximate account of the lateral interactions. In a second step one iteratively refines the model depending on the simulation results one obtains. Due to the non-linearities of the reaction network, such an approach is not fool proof though, i.e. the initial model can be so coarse that it leads into a completely wrong direction. A highly appealing alternative especially for the trajectory-based 1p-kMC simulations would therefore be to only compute the really required reaction barriers on-the-fly, i.e. in the course of the on-going 1p-kMC simulation. Such approaches come with names like adaptive kMC, on-the-fly kMC, self-learning kMC, or kinetic activation-relaxation technique [91–94]. They would indeed also be most appealing from the perspective of a dynamical catalysis picture, as such approaches would not necessarily be restricted to a fixed lattice model. The essential idea of these kind of on-the-fly kMC formulations is to compute all energetically low-lying (and therefore dynamically relevant) barriers out of a given system state α. In accordance with the kMC algorithm, one of the corresponding elementary processes is executed and brings the simulation into a new system state β. This process is then iterated, i.e. barrier calculations are performed sequentially for every new state visited. Huge savings in computational time can thereby be achieved when appropriately storing the already computed barriers and introducing some form of state recognition. If the algorithm thus realizes that the new state β corresponds to an already visited earlier state α, barriers are not recomputed, but drawn from the existing look-up tables. Despite these savings, the computational effort of an at least semi-reliable exploration of all low-lying barriers at individual kMC steps is generally still orders of magnitude higher than those of the traditional divide-and-conquer look-up formulation. Applications of on-the-fly kMC in surface catalysis are therefore presently either restricted to very specialized systems with only reduced configurational complexity or they employ force fields rather than DFT calculations for the process barriers.

The computationally expensive part of an actual barrier calculation is in either case the location of the TS through advanced transition state search algorithms [95, 96]. In on-the-fly 1p-kMC, where the final states are not known, this would be one-ended techniques like the dimer method [97, 98]. In the prevalent divide-and-conquer 1p microkinetic approaches, where initial and final state of an elementary process are known, most accurate results are instead obtained by state-of-the-art two-ended techniques like the (climbing image) nudged elastic band (NEB) method or string approaches [99–101]. Regardless of dimer, NEB, or string, one TS search will involve numerous individual DFT calculations. For the system sizes typical for surface catalytic problems these DFT calculations may furthermore exhibit severe convergence issues, or the actual TS search algorithm has problems converging to

the (right) TS. The barrier determinations are therefore the by far most critical and (human and CPU) time-consuming step in a 1p microkinetic study. Obviously, it is thus also this step that has the highest leverage for speed-ups through more approximate approaches. This starts already with the use of less rigorous TS search algorithms like drag methods or a mere calculation of energy profiles along assumed reaction paths. However, most prominently and with highest efficiency gains, this has been exploited by approximate relations between the activation energies and the thermochemistry of the reaction [102–108]. One prominent example are the well-known Brønsted-Evans-Polanyi (BEP) relationships [5, 7, 106–108], which yield linear relations of the kind $\Delta E_a \approx c_1 (E_f - E_i) + c_2$, where c_1, c_2 are constants and $(E_f - E_i)$ is the energy difference of the initial and final state of the reaction. Since the latter thermochemical energy difference only involves geometry optimizations of (meta)stable configurations, knowledge of such a relation yields substantial reductions in computational cost as compared to an explicit TS search. An even further reduction in cost and the number of independent parameters has been achieved by realizing that the binding energetics of many reaction intermediates can be related to the binding energetics of a few base elements out of which these reaction intermediates are typically composed, namely H, C, N, O, and S [108–110]. While the initial task was thus to explicitly compute a considerable number of energy barriers for each elementary process of the considered reaction network, exploitation of the latter scaling relations and BEP relations may reduce this to the calculation of the binding energies of a few base elements. This can imply such an enormous reduction in the computational cost that it allows to access quite complex reaction networks and in particular engage in computational screening studies [7, 108, 111–119]. This route has hitherto been exclusively pursued within 1p-MF rate equation approaches. As the goal of kMC-based 1p microkinetic modeling is typically more a comprehensive and most accurate understanding of a particular system, use of such more approximate scaling and BEP energetics may have seemed less obvious. However, there is no conceptual obstacle against doing so in the future.

7.3.3 *Surface Morphological Transitions in Near-Ambient Catalysis*

Just as with (constrained) ab initio thermodynamics, a central outcome of 1p microkinetic modeling is the surface structure and composition as a direct function of the surrounding gas phase. As the theory is explicitly time dependent, this can be for steady-state reaction conditions, but equally for non-stationary situations as for example in temperature-programmed-reaction (TPR) experiments. 1p-MF rate equation theory provides this information in the form of average coverages at the considered active sites. 1p-kMC simulations additionally provide the detailed spatial distributions and fluctuations at the surface. Such insight is invaluable to

properly capture and analyze microstructural effects, for instance at oxide surfaces or defects like vacancies or steps. Of course, the 1p-kMC distributions can also be averaged to obtain (proper) average coverages without having to resort to the MF approximation.

In the resulting surface populations the kinetic effects due to the on-going reaction events (that were neglected in constrained ab initio thermodynamics) are now explicitly considered. Also, "phase" transitions are better described as "configurational entropy" is accounted for. In 1p-MF rate equation theory without any coverage dependencies this is at a level equivalent to Langmuir models [120], in 1p-kMC this is the accurate numerical evaluation on the ensemble of active sites considered. Quite deliberately, I have put the words "phase" and "configurational entropy" in quotes here, as these are inherently thermodynamically defined terms, while the consideration of an open catalytic system with on-going reaction events in 1p-kMC and 1p-MF obviously brings us outside the realm of thermodynamics. To reflect this, pioneering kMC work on surface catalytic problems [121] has created the, sometimes critically mocked word "kinetic phase diagrams" (then containing "kinetic phase transitions" etc.) to denote the equivalent compositional output as compiled in the surface phase diagrams of (constrained) ab initio thermodynamics as e.g. shown in Figs. 7.1, 7.2 and 7.3. In the following I will stay within this type of nomenclature in exactly the spirit as put forward by Ziff, Gulari, and Barshad [121].

Figure 7.4 shows such a kinetic phase diagram for the CO oxidation problem at $RuO_2(110)$ that I discussed at the (constrained) ab initio thermodynamics level above. Directly compared are results obtained by 1p-kMC simulations and 1p-MF rate equation theory [60, 78]. Both microkinetic simulations have been based on exactly the same DFT input and the same considered reaction network, such that the differences discernible in Fig. 7.4 arise exclusively from the mean-field approximation in the MF approach. Even though the overall topology of the phase diagram is largely robust against this approximation, the positions of the catalytically most relevant kinetic phase boundaries are somewhat shifted. A detailed analysis shows that this goes hand-in-hand with significant shortcomings of MF theory to appropriately describe the catalytic activity and underlying reaction mechanisms [78]. More important for the present context are, however, the much more significant deviations in the predicted surface structure and composition when comparing both 1p microkinetic theories with the approximate thermodynamic insight in Fig. 7.3. What prevails is the insight that technologically relevant reaction conditions with pressures of the order of 1 atm and near-stoichiometric reactant ratios fall in the vicinity of a phase transition, and in particular the one in which adsorbed O and CO compete for the so-called coordinately unsaturated (cus) sites offered by this surface. This finding and the importance of the cus sites for the catalytic activity of $RuO_2(110)$ are fully consistent with all presently available experimental data [11, 13, 14]. Substantial differences between (constrained) thermodynamic and microkinetic theory are, however, obtained for the population of the other (br) idge active site type offered by the $RuO_2(110)$ surface. While (constrained) ab initio thermodynamics predicts a predominant population with O^{br} even for largely CO-rich gas-phase conditions [37, 59], both microkinetic theories agree on an

essentially complete replacement by CO^{br} species in this regime. This is a classic illustration of the surface catalytic reactions consuming a reaction intermediate, here O^{br}, faster than it can be replenished by adsorption from the gas phase. Since ab initio thermodynamics is blind to such kinetic effects, it only assesses the very strong binding of O to these bridge sites and thereby largely overestimates the presence of this species at the surface.

This showcase example thus nicely underscores the approximate nature of (constrained) ab initio thermodynamics results and the added value of explicit 1p microkinetic theories. Of course, not everything is perfect in the latter theories either. Even in the highly CO-rich gas-phase conditions in the upper left parts of the panels in Fig. 7.4 both 1p microkinetic theories predict at maximum a fully CO-poisoned oxide surface, whereas the thermodynamic estimates in Fig. 7.3 immediately reveal the proper complete reduction of the oxide. This difference arises as the predictive power of the 1p microkinetic approaches extends, of course, only to the active sites and concomitant set of elementary processes considered in the model. In the studies behind Fig. 7.4 this framework corresponded to the active sites of a reduced, but otherwise intact $RuO_2(110)$ surface. The structural complexity that would arise when considering a full oxide reduction path would presently imply a completely intractable 1p input (vide infra), let alone that at best only a conceptual perception of the individual mechanistic steps involved in such a path is available to date [122, 123]. For the targeted CO oxidation activity of $RuO_2(110)$ this limitation with respect to oxide reduction is thereby not actually the real problem. Relevant, near-stoichiometric gas-phase conditions are located sufficiently well inside the stability regime of the bulk oxide, cf. Figs. 7.3 and 7.4. However, a long-term deactivation of this $RuO_2(110)$ facet has been experimentally reported even for oxidizing feeds, which was assigned to a microfaceting into an inactive c (2×2)-$RuO_2(100)$ structure [124]. Again, such a reaction-induced complex

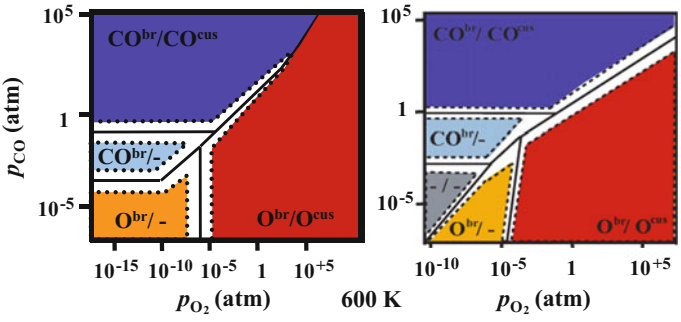

Fig. 7.4 Kinetic surface phase diagrams for the $RuO_2(110)$ surface in an environment consisting of O_2 and CO at 600 K. Compared are results from 1p-kMC simulations (*left panel*) with results from 1p-MF rate equation theory (*right panel*). The labels of the different stable phases reflect a predominant population (O, CO, or empty "–") of the two prominent adsorption sites offered by this surface, br(idge) and coordinatively unsaturated (cus) site. Coexistence regions at the phase boundaries are marked in *white*. Labels and shown ranges of partial pressures (gas-phase chemical potentials) are identical to those in Fig. 7.3. From [60, 78]

surface morphological transition—which is a prototypical example for exactly the dynamical view of an evolving catalyst we would like to scrutinize—is presently largely outside the reach of predictive-quality microkinetic modeling capabilities.

Fortunately, the situation is a bit more accessible for the Pd(100) example discussed before. Due to the reduced stability of bulk PdO, here "only" the (possibly continuous) formation and reduction of a thin surface oxide film while on stream is to be assessed. A first step in this direction has been taken by simply performing 1p-kMC simulations once on the pristine metal, i.e. for a lattice model and set of elementary reactions pertinent to Pd(100), and once on the perfectly intact surface oxide, i.e. for a lattice model and set of elementary reactions pertinent to the $(\sqrt{5} \times \sqrt{5})$R27° surface oxide [87]. Evaluating the average surface composition for a wide range of gas-phase conditions one can assess the boundaries within which one would still trust either of the two models. Detailed experimental work indicates the onset of surface oxide formation once a critical O coverage around and above 0.5 ML on Pd(100) is exceeded [46]. This suggests the 1p-kMC Pd(100) model as a faithful representation for gas-phase conditions where the O coverage stays well below this value. Equivalently, one would expect the onset of surface oxide decomposition whenever a critical coverage of surface oxygen vacancies, say 10%, is exceeded [44]. For gas-phase conditions where this coverage is much lower, the intact 1p-kMC surface oxide model should be a good representation. Intriguingly, the results of the corresponding 1p-kMC simulations shown in Fig. 7.5 identify a finite range of (T, p_{CO}, p_{O2})-conditions where both stability criteria are fulfilled [87]. In this range the Pd(100) 1p-kMC model predicts an O coverage below 0.25 ML, while simultaneously the $(\sqrt{5} \times \sqrt{5})$R27° surface oxide 1p-kMC model predicts a surface oxygen vacancy concentration well below 10%. The corresponding bistability region is thereby quite robust against uncertainties in the DFT energetics or the treatment of lateral interactions. Moreover, its location in (T, p_{O2})-space in fact comprises precisely the near-ambient reaction conditions for

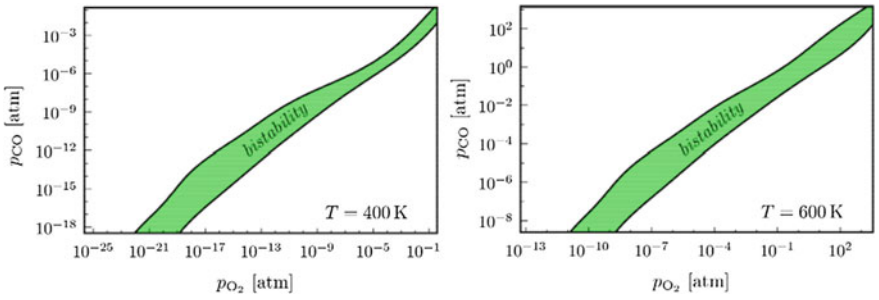

Fig. 7.5 Bistability region in CO oxidation catalysis, i.e. gas-phase conditions where 1p-kMC models simultaneously predict the stability of pristine Pd(100) and the $(\sqrt{5} \times \sqrt{5})$R27° surface oxide. At 600 K this bistability region comprises technologically relevant (near-)ambient, stoichiometric gas-phase conditions. At 400 K this region is shifted to more O-rich conditions as employed in the Reactor STM experiments by Hendriksen et al. [56, 61, 62]. From [87]

which Reactor STM studies had reported an oscillatory formation and decomposition of an oxidic film at the surface of the working catalyst [56, 61, 62].

In particular at elevated temperatures, 600 K in Fig. 7.5, the bistability region centers on technologically most relevant near-stoichiometric partial-pressure ratios. These findings thus fully support a dynamic view of catalysis at least in the sense that a surface morphological transition, here the formation of a thin surface oxide layer, may indeed occur in the reactive environment. The simulations, performed separately on the two intact surface states, can, however, not address whether the very dynamics of the transition itself is a key factor. In other words, whether it is only the continuous formation and decomposition of the oxidic film in the experimentally reported oscillations that creates the real active sites, e.g. in form of transient structures or at domain boundaries on the evolving surface. For this the 1p-kMC simulations would have to be able to represent both surface states and transitions between them. For this very system a step in this direction has in fact recently been taken through a novel multi-lattice kMC approach, which exploits the lattice commensurability of the $(\sqrt{5} \times \sqrt{5})R27°$ surface oxide with the Pd(100) surface [125]. The latter allows to establish a superlattice model that simultaneously comprises both metal and surface oxide sites, with the multi-lattice kMC algorithm keeping track of which surface areas are either in the oxide or the pristine metal state by appropriately activating or deactivating elementary processes at the corresponding sites. At present this approach has only been applied to the reduction of the surface oxide in a CO atmosphere [125]. Intriguingly, CO oxidation reaction steps across metal-oxide domain boundaries turned indeed out to be essential to reproduce the experimentally reported temperature dependence of the reduction rate [126].

Whether the same or other processes related to the dynamics of an evolving surface are also crucial for steady-state CO oxidation catalysis remains yet to be seen. The price to pay for such insight through multi-lattice kMC simulations is to establish a detailed atomistic pathway for the transition between the treated system states, here the pristine metal and the surface oxide. The exploitation of the lattice commensurability renders this endeavor tractable. It nevertheless constitutes a computationally most expensive step involving a multitude of 1p calculations [125]. While this obviously restricts the dynamical phenomena in catalysis that can presently be tackled, an important aspect to keep in mind is the following. Regardless of whether traditional single- or multi-lattice 1p-kMC, already the lattice models and concomitant elementary process lists that can be handled today allow to treat quite complex reaction networks that comprise many different reaction mechanisms. Which of these reaction mechanisms dominates the catalysis is then an output of the simulations, not an input. This is a crucial asset that distinguishes such 1p microkinetic simulations from ubiquitous kinetic studies where a certain reaction mechanism is simply assumed, often based on rather little or only indirect evidence.

7.3.4 Catalytic Activity from First Principles

Another important asset of 1p microkinetic simulations is, of course, that they do not only provide information about the surface structure and composition, but also determine the catalytic activity and, if applicable, the selectivity. Just as much as for the surface (kinetic) phase diagrams this information can be computed in steady state for a range of gas-phase conditions and then be compiled in corresponding, so-called TOF maps. Alternatively, if transient situations are addressed, it can for example be computed for various initial system states. Figure 7.6 shows examples for such data drawing on the previously-discussed example of CO oxidation at $RuO_2(110)$ [127, 128]. In both shown examples the absolute pressures addressed are in the UHV regime, which makes it possible to directly compare to corresponding data from Surface Science experiments (vide infra). In both cases excellent agreement is reached, which in particular for the transient TPR data is only obtained through the appropriate consideration of the spatial distributions at the catalyst surface. As shown in Fig. 7.6 qualitatively different variations with initially prepared O^{cus} coverage would be expected for two competing reaction mechanisms, $O^{br} + CO^{cus}$ (~linear variation) and $O^{cus} + CO^{cus}$ (~parabolic variation). The latter mechanism is known to be the more reactive one due to the much weaker binding of the O^{cus} species. The at first glance enigmatic strong suppression of this mechanism seen in Fig. 7.6 is instead a direct result of diffusion limitations in the trench-like arrangement of the cus sites under the specific experimental TPR conditions. Such an effect can only be captured by 1p-kMC simulations, which only then are able to reconcile the known higher reactivity of the $O^{cus} + CO^{cus}$ mechanism with the linear profile measured in the TPR experiments [128]. Both for this

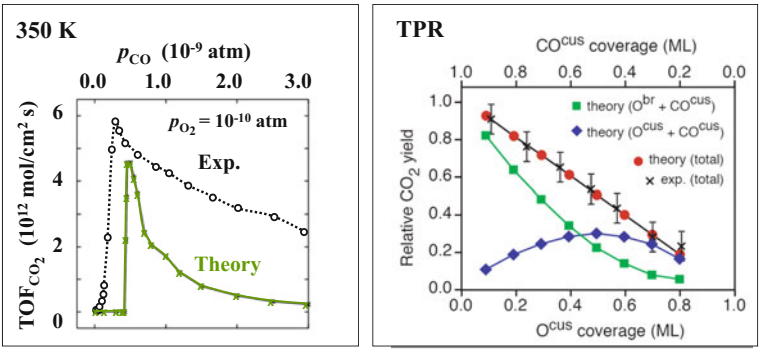

Fig. 7.6 Comparison of measured and 1p-kMC computed steady-state and transient catalytic activity for CO oxidation at $RuO_2(110)$. (*Left*) Steady-state turnover frequencies (TOFs) at 350 K. (*Right*) Total CO_2 yield obtained in TPR spectroscopy for surfaces initially prepared with varying O^{cus} and CO^{cus} coverage. The CO_2 yield is given relative to the one obtained for the surface with zero O^{cus} coverage. Shown are the total simulated CO_2 yield and the contributions from the two dominant reaction mechanisms under these conditions, $O^{cus} + CO^{cus}$ and $O^{br} + CO^{cus}$. From [127, 128]

example and in general, the capability to explicitly resolve the contributions of individual reaction mechanisms to the overall (and observable) catalytic activity is thus a most important aspect for the mechanistic understanding. Obtaining wrong relative contributions correspondingly bears the risk of deducing wrong conclusions (and "ideas"). Similar to the TPR case, a wrong ordering of the contribution from different reaction mechanisms in 1p-MF rate equation theory has also been reported for steady-state reaction conditions [78], which thus adds to the list of shortfalls of this theory if the MF approximation is unjustified.

Despite reports of a number of similarly successful 1p microkinetic studies [113], one has to recognize that reaching a quantitative agreement in absolute TOFs cannot generally be expected. This holds already because of the typically large uncertainties in experimental absolute TOFs. The uncertainties on the theoretical side are not any smaller, primarily due to the aforementioned uncertainties in the approximate DFT energetics. At the temperatures of interest in catalysis, the quoted ~0.3 eV (~30 kJ/mol) uncertainty in DFT barrier values translates into 1p rate constants that can be wrong by several orders of magnitude. For more approximate BEP or scaling-derived barriers, this will be even worse. At first glance such a large uncertainty seems to invalidate any attempt to compute meaningful TOFs, or it lends support to the pragmatic approach to empirically "correct" 1p microkinetic simulations such that they match certain experimental findings [129]. A more constructive approach that does not sacrifice the invaluable independence of a first-principles theory is instead to systematically analyze which errors in the 1p energetic data base can really contribute to what degree to errors in the predicted activity (or other properties of interest). A central concept in this respect are so-called sensitivity analyses, which loosely speaking are nothing but a systematic variation of the input energetic parameters to assess the influence this has on the outcomes of the microkinetic model (surface composition, activity, selectivity, relative contributions of reaction mechanism, etc.) [130–136].

Formulated as linear response theories, approaches like the degree of rate control [131, 135] thereby vary individual rate constants (barriers), while keeping everything else fixed. The insight such analysis provides is which of the elementary processes are rate-controlling (rate-determining) and which ones are not. There are several things one can learn from this. An immediate insight is the corresponding mechanistic understanding about the reaction network per se. This is often much more robust with respect to the DFT uncertainties and in itself typically much more relevant than being able to quantitatively determine an absolute TOF. Among others knowledge of the rate-determining steps is the gateway to simplified descriptions of the reaction network and therewith to computational screening, as much as it identifies those kinetic bottlenecks that need to be addressed in a rational design of improved catalysts. With respect to the DFT uncertainty, rate constants of not- rate-determining processes can typically be varied by several orders of magnitude without having any effect on the simulation result. We correspondingly learn that DFT errors in such rate constants are irrelevant. On the contrary, any error contained in the description of rate-determining steps will directly propagate through and these are then the errors one should worry about.

In some cases knowing which energetic input quantities are the crucial ones already allows to rationalize agreement or disagreement with experimental data. For the steady-state catalytic activity shown in Fig. 7.6 a degree of rate control analysis e.g. reveals that under the probed gas-phase conditions it is primarily the dissociative adsorption of O_2 into a cus site pair that is rate determining [135]. The good agreement with experiment then comes about as this is a non-activated process. Rather than by the possibly inaccurate DFT rate constant, the TOF is in this case controlled by the limited availability of free site pairs for O_2 adsorption which is determined on the statistical-mechanical level. In the general case, sensitivity analyses identify those microscopic input quantities on which attention should be focused, say a particular binding energy or a particular reaction barrier. Benchmark against higher-level theory or experiment can then in principle provide an assessment how much the particular DFT quantity is actually in error, and through the sensitivity analysis how much this propagates through to the absolute TOF. The latter step is important as it tells, whether a deviation between simulated and experimental TOFs is really (exclusively) due to an inaccuracy in the underlying 1p energetics. As I will illustrate further below, there can be multiple other reasons for such deviations. This alone is an important argument against simply empirically "correcting" the microkinetic simulations by fitting selected 1p energetic values to match experimental activities or other meso-/macroscopic observables. Such a fudging can easily mask the true reasons for the deviation between 1p theory and experiment. Also replacing the 1p energetic quantity with a corresponding experimental microscopic benchmark quantity is a dangerous endeavor. Even if experimental quantities carry microscopic names like "adsorption energy" or "reaction barrier" they are typically the result of some approximate data analysis scheme, for which the multitude of TPR analyses represents a prominent example [137]. Rather than clean data, such numbers are thus effective quantities that contain an unspecified systematic error that is not covered by the quoted statistical error bars. Even in case of allegedly direct energetic measurements like microcalorimetry, firmly believed reference numbers do change with time and it remains an ongoing challenge to fully establish a safe experimental database for adsorption energetics [138].

A further argument against selectively replacing individual DFT energetic parameters with empirical numbers are the systematic trends often exhibited by DFT errors, with the widespread PBE functional [139] for instance suspected to show a systematic overbinding at metal surfaces [140]. Replacing individual energetic quantities breaks such trends and thereby a potential compensation of the systematic errors. Such correlations in the underlying energetic data base could also not be captured by the above-described linear-response type sensitivity analyses. In this respect, the concept behind the recently introduced Bayesian error estimation functionals (BEEF) represents an intriguing step forward [141–143]. The idea here is to generate an entire ensemble of functionals where known errors in adsorption energetics are mapped onto uncertainties of the parameters entering the electronic xc model. Rather than once, a 1p microkinetic simulation is then run multiple times, each time with different energetic data sets obtained from an appropriate sampling

of this ensemble of functionals. The spread of the results obtained provides a quantitative error estimate and first applications of this BEEF concept indeed indicate that correlations in the DFT errors significantly reduce the predicted error on calculated TOFs [144].

In fact, an even larger reduction of errors was reported when comparing TOFs calculated for different metal catalysts [144]. This is important as corresponding relative activity comparisons, also of the same catalyst for different reaction conditions, are in any case much more relevant than the computation of an individual absolute TOF for one set of reaction conditions. The increased robustness of such trends could furthermore also rationalize the success of emerging computational screening studies which rest entirely on a comparison of relative activities varying over many orders of magnitude [7, 108, 111–119]. The critical aspect here is therefore likely less the 1p energetic data base, but the rather drastic assumptions on the microkinetic level that are presently made to make such studies tractable. Even through comparing an entire series from early to late transition metals, identical reaction mechanisms are for instance simply imposed (and not evaluated as in 1p-kMC simulations). As discussed at the beginning of this section, these reaction mechanisms furthermore typically only consider a few active sites as offered by a static, bulk-truncated surface. Even though the typically obtained, volcano-shaped activity variations over a transition metal series often exhibit their peaks close to metals that are known to be good catalysts for the studied reaction, it is presently not clear if this should really be seen as a validation of the imposed mechanism. As such it is an open question whether the success of the seminal screening studies has any bearing on the issue of a static versus a dynamically evolving catalyst surface. The true answer will eventually only come from future 1p microkinetic (screening) studies in which the possibility of surface morphological transitions is explicitly contained in the employed model.

7.3.5 Mass Transfer Limitations Under Near-Ambient Conditions

Regardless of the already discussed uncertainties in 1p calculated TOFs, there is yet another complication when comparing them to experiment that particularly applies to the in situ context, i.e. to the quest to specifically address catalytic activities at technologically relevant near-ambient conditions. For corresponding pressures the actual flow of mass and heat through the employed reactor becomes a significant factor. In fact, especially the dedicated experimental setups employed in in situ studies of model catalysts are likely to exhibit most complex flow profiles, as sophisticated spectroscopic probes and pumps often need necessarily to be placed in the direct vicinity of the catalyst surface [8, 9]. For the intrinsically targeted reaction conditions with highest turnovers of reactants into products this can give rise to heat and mass transfer limitations, i.e. significant temperature and (partial) pressure

gradients inside the reactor [16–18, 145]. The local gas-phase composition (and therewith reaction conditions) directly at the catalyst surface may then deviate significantly from the nominal reaction conditions controlled at the inlet of the reactor. Existence of such mass transfer limitations generally prevents any meaningful measurements of the catalytic activity via the standard compositional analysis at a reactor outlet or orifices placed at the reactor walls. They also prevent any straightforward comparison to 1p microkinetic simulations, unless the latter are suitably integrated into a computational framework that appropriately accounts for the concentration and flow profiles in the reactor.

Such an integration into corresponding computational fluid dynamics (CFD) simulations has a longer history for MF rate equation theory [146], but could only recently be achieved for kMC based microkinetic simulations [16–18]. Placed into the context of 1p microkinetic simulations, resulting 1p-MF–CFD or 1p-kMC–CFD multiscale modeling frameworks are in their absolute infancy. For the theme of a potentially dynamically-evolving catalyst surface they nevertheless bear exciting prospects. Up to now this discussion centered only on the possibility of surface morphological transitions at the working catalyst, with in particular the CO oxidation at Pd(100) example pointing at an intrinsic heterogeneity of the surface. This does not answer the central question as to the nature of the active sites. Is one of the coexisting phases much more active than the other, or are active sites maybe only created at the (evolving) phase boundaries? Corresponding answers could be provided by a dedicated analysis of in situ activity data, appropriately accounting for potential flow limitations in the experiment. For the CO oxidation at Pd(100) system such a first analysis of laser-induced fluorescence (LIF) data has in fact already heralded the intriguing contributions this can make [147].

Figure 7.7 shows the LIF-measured CO_2 concentration directly above the catalyst surface, which is a non-invasive local measure of the product formation and therewith of the catalytic activity [147]. Also shown are the corresponding signals as predicted by 1p-kMC–CFD simulations either employing the 1p-kMC lattice model for the pristine Pd(100) surface or the 1p-kMC lattice model for the surface oxide. For the measured range of reaction conditions, namely a temperature ramp at constant pressure and slightly O-rich stoichiometry, only the prior model yields a signature compatible with the experimental data. This suggests the predominant catalytic activity to be due to active sites still being in a metallic surface termination. On the other hand, there is a notable shift of the theoretical signature by ~100 K to lower temperatures. A sensitivity analysis points at the CO oxidation reaction barrier as rate-determining step, and rerunning the simulations on an energetic data base obtained with the less binding RPBE functional [140] indeed brings the theoretical signature into much closer agreement with experiment, cf. Fig. 7.7. In an empirically "correcting" approach one could now attribute the remaining difference to a still deficient RPBE energetics and simply fit the CO oxidation barrier so as to perfectly match the theoretical and experimental LIF profile.

Alternatively, we could recall that the probed reaction conditions fall into the bistability regime discussed above, and both metal and surface oxide phase could

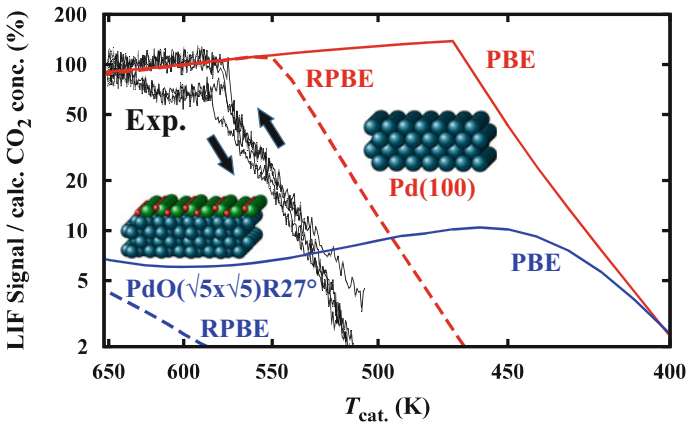

Fig. 7.7 Measured CO_2 LIF signal over the active catalyst surface for a temperature ramp from 500 to 650 K and back (as indicated by the *arrows*). Feed gas conditions are: 4:1 O_2/CO ratio, total pressure 180 mbar; 50% Ar; inlet mass flow 72 ml_n/min. Additionally shown is the corresponding calculated CO_2 concentration variation as predicted for the $(\sqrt{5} \times \sqrt{5})$R27°-O surface oxide (*blue lines*) and for the pristine metal state of Pd(100) (*red lines*). To assess the uncertainties arising from the approximate DFT energetics, data obtained with the PBE [139] (*solid lines*) and RPBE [140] (*dashed lines*) xc functional are shown. From [147]

potentially coexist at the surface [87]. Indeed, at the RPBE level and disregarding any special catalytic activity of sites at domain boundaries, a quantitative agreement with the experimental signature can also be reached when assuming that the predominantly active pristine metal domains cover only a fraction of ~25% of the total surface area [147]. On a methodological level this is a perfect illustration that disagreement of a first-principles theory with experiment can have multiple, quite distinct sources. A naïve fudging of just the 1p energetics to reach agreement in macroscopic observables like catalytic activity is thus ill-advised. Instead, further experiments and/or calculations are required to single out the true source for the disagreement. In the present example, the suggested surface heterogeneity could be scrutinized by combining the LIF activity measurements with an in situ surface characterization technique. If the rationalization in terms of a phase mixture prevails, this could potentially resolve quite some controversies in the emerging field of in situ model catalyst studies. With a prevailing focus on spectro-/microscopic measurements, phases that are predominantly characterized at the working surface have there often tacitly been assumed to also be the ones actuating the catalysis. From a modeling perspective, the truly exciting validation would instead come when multi-lattice or off-lattice kMC simulations are able to explicitly treat an evolving surface heterogeneity. This is the great challenge for the future, and it will for sure create many interesting "ideas" in the context of a reaction-induced dynamical picture of surface catalysis.

7.4 Conclusions and Outlook

Over the last 10–15 years (constrained) ab initio thermodynamics and first-principles microkinetics have become well-established tools in surface catalysis research. (Constrained) ab initio thermodynamics is in fact a routine approach that has spread even well out of academia. It provides first, approximate insight into the structure and composition of the catalyst surface at finite, technologically-relevant gas-phase compositions. Near-term advancement of this technique will most likely center on coupling this thermodynamic framework with global geometry optimization algorithms and thereby overcome the prevalent restricted sampling of configuration space in form of small sets of structural candidates hand-selected by the researcher.

More refined insight into the structure and composition, as well as intrinsic TOFs can be obtained from computationally more involved 1p microkinetic approaches. The power of these techniques and the step-out changes connected with their advent are presently already impressively heralded by trend studies, where rough activity estimates are used for a computational screening of catalyst materials. Such studies are currently based on simplified mean-field kinetic models that assume reaction mechanisms and rate-determining steps, and they employ approximate scaling relations to reduce the required first-principles energetic input. At this level of theory obtaining a detailed mechanistic understanding and quantitative TOFs of an individual system is neither intended, nor achievable. In fact, already the uncertainty in presently-available DFT energetics for extended surface systems will generally prevent reaching quantitative absolute TOFs in the foreseeable future. However, considering that reaching such numbers is similarly elusive in experimental studies this is also not really a goal to worry about. Important is, instead, to systematically validate, e.g. through sensitivity analysis, that the relevant (mechanistic and activity) conclusions drawn are robust with respect to these and other methodological uncertainties.

Due to the continuously increasing computer power alone we will certainly see a rapid spreading of 1p microkinetic modeling in the next years, eventually also into industry. Obvious advancements are the extension to more complex reaction networks with ever diminishing assumptions on reaction paths and intermediates, the move from presently-studied individual facets to entire (supported) nanoparticles, and a gradual shift from prevalent mean-field kinetics to spatially-resolved kinetic Monte Carlo simulations. The central challenge to all of this is that all of the here discussed methodology relies inherently on a rather rigid picture of the catalyst substrate, exploiting a certain level of crystalline order and static active site structures. Addressing the highly dynamic picture of heterogeneous catalysis increasingly suggested by in situ studies—with reaction-induced complex (surface) morphological changes and an evolving, possibly liquid-like phase behavior—is largely impossible with currently available methodology. Great care has to be taken that this incapability to describe such scenarios with present models does not generate the “idea” to readily dismiss them. Instead, it should be a source of motivation to further push the field and tackle the methodological frontiers.

Acknowledgements I am as ever indebted to my research group. Their creativity, curiosity, and enthusiasm for research is my daily motivation. Their diligence, unselfishness, and idealism is the imperative to never lower the pace. I also gratefully acknowledge my temporary second home, the SUNCAT Center at Stanford University. Spending a sabbatical in this stimulating environment has been ideal to assemble the thoughts for this review. This chapter has also been published as Catalysis Letters 146 (3), 541—563 (2016).

References

1. G. Ertl, *Reactions at Solid Surfaces* (Wiley, Hoboken, NJ, 2010)
2. G.A. Somorjai, Y. Li, Proc. Natl. Acad. Sci. U.S.A. **108**, 917–924 (2011)
3. M.A. Newton, Chem. Soc. Rev. **37**, 2644–2657 (2008)
4. R. Schlögl, Angew. Chem. Int. Ed. **54**, 3465–3520 (2015)
5. I. Chorkendorff, H. Niemantsverdriet, *Concepts of Modern Catalysis and Kinetics* (Wiley-VCH, Weinheim, 2003)
6. R.A. van Santen, M. Neurock, *Molecular Heterogeneous Catalysis: A Conceptual and Computational Approach* (Wiley-VCH, Weinheim, 2006)
7. J.K. Nørskov, F. Studt, F. Abild-Pedersen, T. Bligaard, *Fundamental Concepts in Heterogeneous Catalysis* (Wiley, Hoboken, NJ, 2014). ISBN 978-1-118-88895-7
8. A. Stierle, A. Molenbroek, MRS Bull. **32**, 1001–1009 (2007)
9. Ziegler A, Graafsma H, Zhang XF, Frenken JWM (eds) *In-situ Materials Characterization: Across Spatial and Temporal Scales* (Springer, Berlin, 2014)
10. K. Reuter, Oil Gas Sci. Technol. **61**, 471–477 (2006)
11. K. Reuter, Nanometer and sub-nanometer thin oxide films at surfaces of late transition metals. in *Nanocatalysis*, eds. by U. Heiz, U. Landman (Springer, Berlin, 2006). ISBN 978-3-540-32645-8
12. E. Lundgren, A. Mikkelsen, J.N. Andersen, G. Kresse, M. Schmid, P. Varga, Phys.: Condens. Matter **18**, R481–R499 (2006)
13. H. Over, Chem. Rev. **112**, 3356–3426 (2012)
14. J.F. Weaver, Chem. Rev. **113**, 4164–4215 (2013)
15. J. Meyer, K. Reuter, Angew. Chem. Int. Ed. **53**, 4721–4724 (2014)
16. S. Matera, K. Reuter, Catal. Lett. **133**, 156–159 (2009)
17. S. Matera, K. Reuter, Phys. Rev. B **82**, 085446 (2010)
18. S. Matera, M. Maestri, A. Cuoci, K. Reuter, ACS Catal. **4**, 4081–4092 (2015)
19. M.K. Sabbe, M.-F. Reyniers, K. Reuter, Catal. Sci. Technol. **2**, 2010–2024 (2012)
20. K. Reuter, Catal. Lett. **146**, 541–563 (2016)
21. A.F. Voter, Introduction to the Kinetic Monte Carlo Method, in *Radiation Effects in Solids*, ed. by K.E. Sickafus, E.A. Kotomin, B.P. Uberuaga (Springer, Berlin, 2007)
22. K. Reuter, First-Principles Kinetic Monte Carlo Simulations for Heterogeneous Catalysis: Concepts, Status and Frontiers, in *Modelling and Simulation of Heterogeneous Catalytic Reactions: From the Molecular Process to the Technical Syst*em, (Wiley-VCH, Weinhein, 2013). ISBN-10: 3-527-32120-9
23. R.M. Martin, *Electronic-Structure: Basic Theory and Practical Methods* (Cambridge University Press, Cambridge, 2004)
24. K. Burke, J. Chem. Phys. **136**, 150901 (2012)
25. E.A. Carter, Science **321**, 800–803 (2008)
26. P.J. Feibelman, Top. Catal. **53**, 417–422 (2010)
27. C.M. Weinert, M. Scheffler, Mat. Sci. Forum **10–12**, 25–30 (1986)
28. E. Kaxiras, Y. Bar-Yam, J.D. Joannopoulos, K.C. Pandey, Phys. Rev. B **35**, 9625–9635 (1987)

29. M. Scheffler, Thermodynamic Aspects of Bulk and Surface Defects—First-Principles Calculations, in *Physics of Solid Surfaces—1987*, ed. by J. Koukal (Elsevier, Amsterdam, 1987)
30. M. Scheffler, J. Dabrowski, Phil. Mag. A **58**, 107–121 (1988)
31. G.X. Qian, R.M. Martin, D.J. Chadi, Phys. Rev. B **38**, 7649–7663 (1988)
32. X.G. Wang, W. Weiss, S.K. Shaikhutdinov, M. Ritter, M. Petersen, F. Wagner, R. Schlögl, M. Scheffler, Phys. Rev. Lett. **81**, 1038–1041 (1998)
33. X.G. Wang, A. Chaka, M. Scheffler, Phys. Rev. Lett. **84**, 3650–3653 (2000)
34. K. Reuter, M. Scheffler, Phys. Rev. B **65**, 035406 (2001)
35. Z. Lodzianan, J.K. Nørskov, P. Stoltze, J. Chem. Phys. **118**, 11179–11188 (2003)
36. D.A. Mc Quarrie, *Statistical Mechanics* (Harper and Row, New York, 1976)
37. K. Reuter, M. Scheffler, Phys. Rev. B **68**, 045407 (2003)
38. S. Tull, H. Prophet, *JANAF Thermochemical Tables*, 2nd edn. (U.S. National Bureau of Standards, Washington, D.C, 1971)
39. Q. Sun, K. Reuter, M. Scheffler, Phys. Rev. B **67**, 205424 (2003)
40. Q. Sun, K. Reuter, M. Scheffler, Phys. Rev. B **70**, 235402 (2004)
41. D. Loffreda, Surf. Sci. **600**, 2103–2112 (2006)
42. E. Lundgren, J. Gustafson, A. Mikkelsen, J.N. Andersen, A. Stierle, H. Dosch, M. Todorova, J. Rogal, K. Reuter, M. Scheffler, Phys. Rev. Lett. **92**, 046101 (2004)
43. J. Rogal, K. Reuter, M. Scheffler, Phys. Rev. Lett. **98**, 046101 (2007)
44. J. Rogal, K. Reuter, M. Scheffler, Phys. Rev. B **77**, 155410 (2008)
45. G. Zheng, E.I. Altman, Surf. Sci. **504**, 253–270 (2002)
46. S.-L. Chang, P.A. Thiel, J. Chem. Phys. **88**, 2071–2082 (1988)
47. K. Reuter, M. Scheffler, Appl. Phys. A **78**, 793–798 (2004)
48. M. Todorova, E. Lundgren, V. Blum, A. Mikkelsen, S. Gray, M. Borg, J. Gustafson, J. Rogal, K. Reuter, J.N. Andersen, M. Scheffler, Surf. Sci. **541**, 101–112 (2003)
49. P. Kostelník, N. Seriani, G. Kresse, A. Mikkelsen, E. Lundgren, V. Blum, T. Šikola, P. Varga, M. Schmid, Surf. Sci. **601**, 1574–1581 (2007)
50. J. Gustafson, A. Mikkelsen, M. Borg, E. Lundgren, L. Köhler, G. Kresse, M. Schmid, P. Varga, J. Yuhara, X. Torrelles, C. Quiros, J.N. Andersen, Phys. Rev. Lett. **92**,126102 (2004)
51. E. Lundgren, G. Kresse, C. Klein, M. Borg, J.N. Andersen, M. De Santis, Y. Gauthier, C. Konvicka, M. Schmid, P. Varga, Phys. Rev. Lett. **88**, 246103 (2002)
52. A. Michaelides, K. Reuter, M. Scheffler, J. Vac. Sci. Technol., A **23**, 1487–1497 (2005)
53. M.D. Ackermann, T.M. Pedersen, B.L. Hendriksen, O. Robach, S.C. Bobaru, I. Popa, C. Quiros, H. Kim, B. Hammer, S. Ferrer, J.W. Frenken, Phys. Rev. Lett. **95**, 255505 (2005)
54. J. Schnadt, A. Michaelides, J. Knudsen, R.T. Vang, K. Reuter, E. Laegsgaard, M. Scheffler, F. Besenbacher, Phys. Rev. Lett. **96**, 146101 (2006)
55. D.J. Miller, H. Öberg, S. Kaya, H. Sanchez Casalongue, D. Friebel, T. Anniyev, H. Ogasawara, H. Bluhm, L.G.M. Pettersson, A. Nilsson, Phys. Rev. Lett. **107**, 195502 (2011)
56. B. Hendriksen, S. Bobaru, J. Frenken, Surf. Sci. **552**, 229–242 (2004)
57. M. Shipilin, J. Gustafson, C. Zhang, L.R. Merte, A. Stierle, U. Hejral, U. Ruett, O. Gutowski, M. Skoglundh, P.A. Carlsson, E. Lundgren, J. Phys. Chem. C **119**, 15469–15476 (2015)
58. C.T. Campbell, Phys. Rev. Lett. **96**, 066106 (2006)
59. K. Reuter, M. Scheffler, Phys. Rev. Lett. **90**, 046103 (2003)
60. K. Reuter, M. Scheffler, Phys. Rev. B **73**, 045433 (2006)
61. B. Hendriksen, S. Bobaru, J. Frenken, Catal. Today **105**, 234–243 (2005)
62. A. Böttcher, H. Niehus, S. Schwegmann, H. Over, G. Ertl, J. Phys. Chem. B **101**, 11185–11191 (1997)
63. H. Over, Y.D. Kim, A.P. Seitsonen, S. Wendt, E. Lundgren, M. Schmid, P. Varga, A. Morgante, G. Ertl, Science **287**, 1474–1476 (2000)
64. S.J. Roosendahl, A.M. Vredenberg, F.H.P.M. Habraken, Phys. Rev. Lett. **84**, 3366–3369 (2000)

65. R. Kaischew, Commun. Bulg. Acad. Sci. **1**, 100–139 (1950)
66. R. Kaischew, Bull. Acad. Sci. Bulg. **2**, 191–204 (1951)
67. J. Rogal, K. Reuter, M. Scheffler, Phys. Rev. B **69**, 075421 (2004)
68. T. Wang, J. Jelic, D. Rosenthal, K. Reuter, Chem. Cat. Chem. **5**, 3398–3403 (2013)
69. R. Ouyang, J.X. Liu, W.X. Li, J. Am. Chem. Soc. **135**, 1760–1771 (2013)
70. M. Garcia-Mota, M. Rieger, K. Reuter, J. Catal. **321**, 1–6 (2015)
71. C.W. Gardiner, *Handbook of Stochastic Methods* (Springer, Berlin, 2003)
72. G.F. Froment, Catal. Rev. Sci. Eng. **47**, 83–124 (2005)
73. M.J. Hoffmann, S. Matera, K. Reuter, Comp. Phys. Commun. **185**, 2138–2150 (2014)
74. E.W. Hansen, M. Neurock, Chem. Eng. Sci. **54**, 3411–3421 (1999)
75. M. Stamatakis, D.G. Vlachos, J. Chem. Phys. **134**, 214115 (2011)
76. B. Temel, H. Meskine, K. Reuter, M. Scheffler, H. Metiu, J. Chem. Phys. **126**, 204711 (2007)
77. S. Matera, H. Meskine, K. Reuter, J. Chem. Phys. **134**, 064713 (2011)
78. D.J. Liu, A. Garcia, J. Wang, D.M. Ackerman, C.J. Wang, J.W. Evans, Chem. Rev. **115**, 5979–6050 (2015)
79. J.T. Hirvi, T.J.J. Kinnunen, M. Suvanto, T.A. Pakkanen, J.K. Nørskov, J. Chem. Phys. **133**, 084704 (2010)
80. D. Frenkel, B. Smit, *Understanding Molecular Simulation*, 2nd edn. (Academic Press, San Diego, 2002)
81. P. Hänggi, P. Talkner, M. Borkovec, Rev. Mod. Phys. **62**, 251–341 (1990)
82. J.A. Dumesic, D.F. Rudd, L.M. Aparicio, J.E. Rekoske, A.A. Trevin, *The Microkinetics of Heterogeneous Catalysis, American Chemical Society* (1998)
83. S. Müller, J. Phys.: Condens. Matter **15**, R1429–R1500 (2003)
84. Y. Zhang, V. Blum, K. Reuter, Phys. Rev. B **75**, 235406 (2007)
85. M.J. Hoffmann, K. Reuter, Top. Catal. **57**, 159–170 (2014)
86. C. Wu, D. Schmidt, C. Wolverton, W. Schneider, J. Catal. **286**, 88–94 (2012)
87. L.C. Grabow, B. Hvolbaek, J.K. Nørskov, Top. Catal. **53**, 298–310 (2010)
88. A.C. Lausche, A.J. Medford, T.S. Khan, Y. Xu, T. Bligaard, F. Abild-Pedersen, J.K. Nørskov, F. Studt, J. Catal. **307**, 275–282 (2013)
89. G. Henkelman, H. Jonsson, J. Chem. Phys. **115**, 9657–9666 (2001)
90. J.L. Bocquet, Defect diffus. Forum **203**, 81–112 (2002)
91. O. Trushin, A. Karim, A. Kara, T.S. Rahman, Phys. Rev. B **72**, 115401 (2005)
92. F. El-Mellouhi, N. Mousseau, L.J. Lewis, Phys. Rev. B **78**, 153202 (2008)
93. G. Henkelman, G. Johannesson, H. Jonsson, Methods for Finding Saddle Points and Minimum Energy Paths, in *Progress on Theoretical Chemistry and Physics*, ed. by S.D. Schwarz (Kluwer, New York, 2000)
94. H.P. Hratchian, H.B. Schlegel, Finding Minima, Transition States and Following Reaction Pathways on ab initio Potential Energy Surfaces, in *Theory and Applications in Computational Chemistry: The First Forty Years*, ed. by C. Dykstra, G. Frenking, K. Kim, G. Scuseria (Elsevier, Amsterdam, 2005)
95. G. Henkelman, H. Jonsson, J. Chem. Phys. **111**, 7010–7022 (1999)
96. A. Heyden, A.T. Bell, F.J. Keil, J. Chem. Phys. **123**, 224101 (2005)
97. H. Jonsson, G. Mills, K.W. Jacobsen, Nudged Elastic Band Method for Finding Minimum Energy Paths of Transitions, in *Classical and Quantum Dynamics in Condensed Phase Simulations*, ed. by B.J. Berne, G. Cicotti, D.F. Coker (World Scientific, New Jersey, 1998)
98. G. Henkelman, B.P. Uberuaga, H. Jonsson, J. Chem. Phys. **113**, 9901–9904 (2000)
99. E. Weinan, W. Ren, E. Vanden-Eijnden Phys. Rev. B **66,** 052301 (2002)
100. E. Shustorovich, H. Sellers, Surf. Sci. Rep. **31**, 5–119 (1998)
101. E. Hansen, M. Neurock, Surf. Sci. **441**, 410–424 (1999)
102. M. Maestri, K. Reuter, Angew. Chem. Int. Ed. **50**, 1194–1197 (2011)
103. A. Michaelides, Z.P. Liu, C.J. Zhang, A. Alavi, D.A. King, P. Hu, J. Am. Chem. Soc. **125**, 3704–3705 (2003)

104. A. Logadottir, T.H. Rod, J.K. Nørskov, B. Hammer, S. Dahl, C.J.H. Jacobsen, J. Catal. **197**, 229–231 (2001)
105. C.J.H. Jacobsen, S. Dahl, B.S. Clausen, S. Bahn, A. Logadottir, J.K. Nørskov, J. Am. Chem. Soc. **123**, 8404–8405 (2001)
106. H. Toulhoat, P. Raybaud, J. Catal. **216**, 63–72 (2003)
107. S. Linic, J. Jankowiak, M.A. Barteau, J. Catal. **224**, 489–493 (2004)
108. J. Greeley, M. Mavrikakis, Nature Mat. **3**, 810–815 (2004)
109. M.P. Andersson, T. Bligaard, A. Kustov, K.E. Larsen, J. Greeley, T. Johannessen, H. Chris-tensen, J.K. Nørskov, J. Catal. **239**, 501–506 (2006)
110. R.I. Masel, *Principles of Adsorption and Reaction on Solid Surfaces* (Wiley, New York, 1996)
111. R.M. Ziff, E. Gulari, Y. Barshad, Phys. Rev. Lett. **56**, 2553–2556 (1986)
112. K. Reuter, C. Stampfl, M.V. Ganduglia-Pirovano, M. Scheffler, Chem. Phys. Lett. **352**, 311–317 (2002)
113. K. Reuter, M.V. Ganduglia-Pirovano, C. Stampfl, M. Scheffler, Phys. Rev. B **65**, 165403 (2002)
114. F. Abild-Pedersen, J. Greeley, F. Studt, J. Rossmeisl, T.R. Munter, P.G. Moses, E. Skulason, T. Bligaard, J.K. Nørskov, Phys. Rev. Lett. **99**, 016105 (2007)
115. J. Aßmann, D. Crihan, M. Knapp, E. Lundgren, E. Löffler, M. Muhler, V. Narkhede, H. Over, M. Schmid, A.P. Seitsonen, P. Varga, Angew. Chem. Int. Ed. **44**, 917–920 (2005)
116. M.J. Hoffmann, M. Scheffler, K. Reuter, ACS Catal. **5**, 1199–1209 (2015)
117. V.R. Fernandes, J. Gustafson, I.C.H. Svenum, M.H. Farstad, L.E. Walle, S. Blomberg, E. Lundgren, A. Borg, Surf. Sci. **621**, 31–39 (2014)
118. K. Reuter, D. Frenkel, M. Scheffler, Phys. Rev. Lett. **93**, 116105 (2004)
119. M. Rieger, J. Rogal, K. Reuter, Phys. Rev. Lett. **100**, 016105 (2008)
120. K.S. Exner, F. Hess, H. Over, A.P. Seitsonen, Surf. Sci. **640**, 165–180 (2015)
121. M. Boudart, K. Tamaru, Catal. Lett. **9**, 15–22 (1991)
122. C.T. Campbell, Top. Catal. **1**, 353–366 (1994)
123. J.A. Dumesic, J. Catal. **185**, 496–505 (1999)
124. A. Baranski, Solid State Ionics **117**, 123–128 (1999)
125. C. Stegelmann, A. Andreasen, C.T. Campbell, J. Am. Chem. Soc. **131**, 13563 (2009)
126. H. Meskine, S. Matera, M. Scheffler, K. Reuter, H. Metiu, Surf. Sci. **603**, 1724–1730 (2009)
127. M. Kozuch, J.M.L. Martin, Chem. Phys. Chem. **12**, 1413–1418 (2011)
128. D.P. Woodruff, T.A. Delchar, *Modern Techniques of Surface Science* (Cambridge University Press, Cambridge, 1994)
129. J. Wellendorff, T.L. Silbaugh, D. Garcia-Pintos, J.K. Nørskov, T. Bligaard, F. Studt, C.T. Campbell, Surf. Sci. **640**, 36–44 (2015)
130. J.P. Perdew, K. Burke, M. Ernzerhof, Phys. Rev. Lett. **77**, 3865–3868 (1996)
131. J.K. Nørskov, F. Abild-Pedersen, F. Studt, T. Bligaard, Proc. Natl. Acad. Sci. U. S. A. **108**, 937–943 (2011)
132. D. Loffreda, F. Delbecq, F. Vigne, P. Sautet, Angew. Chem. Int. Ed. **48**, 8978–8980 (2009)
133. T. Bligaard, J.K. Nørskov, S. Dahl, J. Matthiesen, C.H. Christensen, J. Sehested, J. Catal. **224**, 206–217 (2004)
134. J.K. Nørskov, T. Bligaard, J. Rossmeisl, C.H. Christensen, Nature Chem. **1**, 37–46 (2009)
135. F. Besenbacher, I. Chorkendorff, B.S. Clausen, B. Hammer, A.M. Molenbroek, J.K. Nørskov, I. Stensgaard, Science **279**, 1913–1915 (1998)
136. B. Hammer, L.B. Hansen, J.K. Nørskov, Phys. Rev. B **59**, 7413–7421 (1999)
137. J.J. Mortensen, K. Kaasbjerg, S.L. Frederiksen, J.K. Nørskov, J.P. Sethna, K.W. Jacobsen, Phys. Rev. Lett. **95**, 216401 (2005)
138. J. Wellendorff, K.T. Lundgaard, A. Møgelhøj, V. Petzold, D.D. Landis, J.K. Nørskov, T. Bligaard, K.W. Jacobsen, Phys. Rev. B **85**, 235149 (2012)
139. B.L.M. Hendriksen, M.D. Ackermann, R. van Rijn, D. Stoltz, I. Popa, O. Balmes, A. Resta, D. Wermeille, R. Felici, S. Ferrer, J.W.M. Frenken, Nature Chem. **2**, 730–734 (2010)
140. A.T. Fromhold, *Theory of Metal Oxidation*, vols. I, II, (North-Holland, Amsterdam, 1976)

141. R.A. van Santen, M. Neurock, S.G. Shetty, Chem. Rev. **110**, 2005–2048 (2010)
142. J.K. Nørskov, T. Bligaard, A. Logadottir, S. Bahn, L.B. Hansen, M. Bollinger, H. Bengaard, B. Hammer, Z. Sljivancanin, M. Mavrikakis, Y. Xu, S. Dahl, C.J.H. Jacobsen, J. Catal. **209**, 275–279 (2002)
143. J. Wellendorff, K.T. Lundgaard, K.W. Jacobsen, T. Bligaard, J. Chem. Phys. **140**, 144107 (2014)
144. A.J. Medford, J. Wellendorff, A. Vojvodic, F. Studt, F. Abild-Pedersen, K.W. Jacobsen, T. Bligaard, J.K. Nørskov, Science **345**, 197–200 (2014)
145. S. Blomberg, M.J. Hoffmann, J. Gustafson, N.M. Martin, V.R. Fernandes, A. Borg, Z. Liu, R. Chang, S. Matera, K. Reuter, E. Lundgren, Phys. Rev. Lett. **110**, 117601 (2013)
146. V.M. Janardhanan, O. Deutschmann Computational Fluid Dynamics of Catalytic Reactors, in *Modelling and Simulation of Heterogeneous Catalytic Reactions: From the Molecular Process to the Technical System*, ed. by O. Deutschmann (Wiley-VCH, Weinheim, 2013). ISBN-10: 3-527-32120-9
147. S. Matera, S. Blomberg, M.J. Hoffmann, J. Zetterberg, J. Gustafson, E. Lundgren, K. Reuter, ACS Catal. **5**, 4514–4518 (2015)